RSC Advances

PAPER

View Article Online
View Journal | View Issue

Cite this: *RSC Adv.*, 2024, **14**, 14051

Novel isatin–triazole based thiosemicarbazones as potential anticancer agents: synthesis, DFT and molecular docking studies†

Alia Mushtaq,[a] Rabbia Asif,[a] Waqar Ahmed Humayun[b] and Muhammad Moazzam Naseer *[a]

Received 13th March 2024
Accepted 23rd April 2024

DOI: 10.1039/d4ra01937g

rsc.li/rsc-advances

Thiosemicarbazones of isatin have been found to exhibit versatile bioactivities. In this study, two distinct types of isatin–triazole hybrids **3a** and **3b** were accessed *via* copper-catalyzed azide–alkyne cycloaddition reaction (CuAAC), together with their mono and bis-thiosemicarbazone derivatives **4a–h** and **5a–h**. In addition to the characterization by physical, spectral and analytical data, a DFT study was carried out to obtain the optimized geometries of all thiosemicarbazones. The global reactivity values showed that among the synthesized derivatives, **4c**, **4g** and **5c** having nitro substituents are the most soft compounds, with compound **5c** having the highest electronegativity and electrophilicity index values among the synthesized series, thus possessing strong binding ability with biomolecules. Molecular docking studies were performed to explore the inhibitory ability of the selected compounds against the active sites of the anticancer protein of phosphoinositide 3-kinase (PI3K). Among the synthesized derivatives, 4-nitro substituted bisthiosemicarbazone **5c** showed the highest binding energy of -10.3 kcal mol^{-1}. These findings demonstrated that compound **5c** could be used as a favored anticancer scaffold *via* the mechanism of inhibition against the PI3K signaling pathways.

1. Introduction

Heterocyclic scaffolds are important synthetic precursors for a wide range of biologically active compounds.[1] They play an important role as a core moiety in a diverse range of natural products, including hemoglobin, biomolecules, RNA, DNA, proteins, vitamins, and biologically active compounds.[2] Isatin (1*H* indole-2,3-dione) has attracted the interest of researchers in both synthetic and medicinal chemistry due to its chemical reactivity and broad range of applications, which include antimicrobial,[3,4] anti-cancer,[5,6] anti-HIV,[7] anticonvulsant,[8] antioxidant,[9,10] anti-inflammatory,[3,11] antitubercular,[12–14] and antidiabetic[11,15,16] properties. Sutent (SU11248), also known as Sunitinib, is a drug derived from 5-fluoro isatin that is used for targeted therapy in gastrointestinal stromal tumors, advanced renal cancer, and pancreatic neuroendocrine carcinoma.[17,18] Fig. 1 shows some biologically active compounds containing isatin scaffold that have been recently reported for their anticancer potential.[19–21]

Triazoles, specifically 1,2,3-triazole and 1,2,4-triazole, stand out as highly significant nitrogen-containing heterocycles. The incorporation of triazole can enhance solubility and facilitate binding to biomolecular targets through a range of non-covalent interactions.[22] Triazoles exhibit a broad spectrum of biological activities, encompassing antimicrobial,[23] antiviral,[24] analgesic,[25] anti-inflammatory,[26] antileishmanial,[26,27] and anticancer[28,29] activities. The development of resistance to drugs used to treat different diseases is a serious problem which needs to be addressed.[30] Hence, extensive efforts have been made for the synthesis of safe, more effective, selective and multi-targeted drugs by utilizing pharmacophore hybridization approach.[31,32] Several *N*-1,2,3-triazole–isatin hybrids have been reported for their potential as tumour anti-proliferative,[33,34] antitubercular,[13,35] and antimicrobial[36] agents. Furthermore, thiosemicarbazones (TSCs) being a type of Schiff bases (typically synthesized by condensation of thiosemicarbazides with a suitable aldehyde or ketone)[37] have also captured the interest of the chemical and biological communities owing to their potent metal chelating ability and diverse pharmacological effects.[38,39] TSCs have displayed a broad clinical antitumor spectrum, with efficacy against leukemia, pancreatic cancer, breast cancer, non-small cell lung cancer, cervical cancer, prostate cancer, and bladder cancer.[38,40–48]

The strategy of linking two pharmacophores together in order to improve the biological and pharmacological potency of the resulting molecules is now widely used in pharmaceutical

[a]*Department of Chemistry, Quaid-i-Azam University, Islamabad 45320, Pakistan. E-mail: moazzam@qau.edu.pk*

[b]*Department of Medical Oncology & Radiotherapy, King Edward Medical University, Lahore 54000, Pakistan*

† Electronic supplementary information (ESI) available. See DOI: https://doi.org/10.1039/d4ra01937g

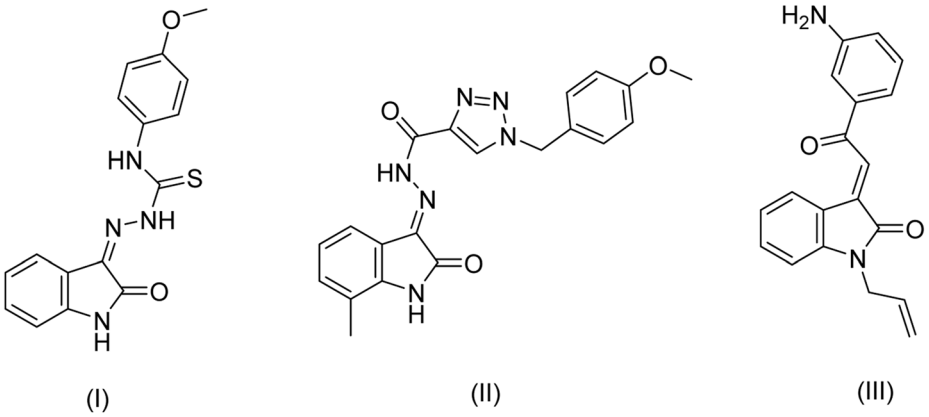

Fig. 1 Some biologically active isatin derivatives as anticancer agents.[19–21]

and medicinal chemistry.[49] When compared to individual moieties, this pharmacophore hybridization approach holds promise for overcoming drug-resistance and increasing potency. Motivated by these considerations and our desire to find more potent anticancer agents to combat drug resistance, we present a facile synthetic protocol for synthesizing novel mono and bis-thiosemicarbazone derivatives of isatin–triazole hybrids through the well known Cu(I)-catalyzed alkyne–azide cycloaddition (CuAAC) reaction. In the present study, the DFT studies of all the synthesized compounds have been explored in order to forecast the structure–reactivity relationship of the synthesized compounds. The most reactive compounds among the series, having the least band gap energy have been selected for the molecular docking studies and explored their probable binding interactions with phosphoinositide 3-kinases (PI3K) which is one of the key therapeutic targets for cancer treatment. The results of this study clearly indicate the potential of the synthesized compounds as anticancer agents, thus providing important guidelines for *in vitro* and *in vivo* studies of the synthesized compounds and for the design and development of efficient anticancer agents. It is also worth mentioning here that a considerable number of clinically approved anticancer drugs either in current use or undergoing trials are derived from isatin, 1,2,3-triazoles and thiosemicarbazones.[50–54]

2. Results and discussion

2.1 Synthesis

The synthesis of two distinct types of desired isatin–triazole hybrid intermediates **3a** and **3b** was initiated from the terminal alkynes **1b** and **2a** (Scheme 1), both of which were prepared *via* *N*-propargylation of commercially available isatin and 4-hydroxybenzaldehyde respectively with the propargyl bromide in the presence of K_2CO_3 in DMF.[55] The targeted alkynes, 1-(prop-2-ynyl)indoline-2,3-dione **1b** and 4-(prop-2-ynyloxy) benzaldehyde **2a** were obtained after recrystallization from ethanol as brown and orange color precipitates in appreciable yield of 92% and 84%, respectively (Scheme 1). Similarly, the azide precursors **1a** and **2b** were synthesized in good yields of 92% and 78% from intermediates 1-(2-chloroethyl)isatin and 4-(2-chloroethoxy)benzaldehyde respectively,[56] by their reaction with sodium azide. Finally, the conditions of "Click" chemistry *i.e.* Cu(I) catalyzed 1,3-dipolar cycloaddition reaction (CuAAC)[55] was employed to synthesize isatin–triazole hybrid intermediates **3a** and **3b**. The reaction between the respective alkynes **1b** and **2a** and the azide precursors **1a** and **2b** in the presence of copper sulphate as a catalyst and sodium ascorbate as a reducing agent for copper sulphate provided the desired isatin–triazole hybrid intermediates **3a** and **3b** in 89% and 85% yield, respectively (Scheme 1).

In the next step, series of mono and bis-thiosemicarbazones **4a–h** and **5a–h** (Scheme 2) were synthesized from isatin–triazole hybrid intermediates **3a** and **3b** by using suitable N^4-substituted thiosemicarbazides in different stoichiometric ratios. The synthesis of mono-thiosemicarbazone derivatives **4a–h** was achieved by stirring **3a** and respective N^4-substituted thiosemicarbazide (1.1 eq.) for 4–8 h in ethanol solvent at room temperature. Similarly, bis-thiosemicarbones of isatin–triazole hybrids **5a–h** were obtained by reacting **3a** and **3b** with 2.1 equivalents of suitable N^4-substituted thiosemicarbazide under reflux conditions (Scheme 2).

2.2 Characterization

The formation of isatin–triazole hybrid intermediates **3a** & **3b** and mono and bis-thiosemicarbazones **4a–h** & **5a–h** was confirmed by their FT-IR, ^{1}H & ^{13}C NMR and LC-MS data. In the FT-IR spectrum, the absence of the absorption peaks for azide and alkyne functional groups and the presence of three absorption bands at (1732 cm^{-1}, 1692 cm^{-1} and 1598 cm^{-1}) and (1728 cm^{-1}, 1673 cm^{-1} and 1600 cm^{-1}) corresponding to the three carbonyls of the lactam, aldehyde and ketone functional groups clearly indicate the successful formation of intermediates **3a** & **3b**, respectively. Moreover, the presence of absorption bands for ether, methylene and aromatic rings in their respective regions also establishes the desired structures.

In the ^{1}H NMR spectrum, the only singlet present in the aromatic region at 8.25 ppm and 7.85 ppm, respectively corresponds to the single proton of triazole ring of **3a** & **3b**. The presence of two triplets in ^{1}H NMR of **3a** at 4.30 ppm ($^3J = 6$ Hz) and 4.84 ppm ($^3J = 6$ Hz) for two methylene protons attached to

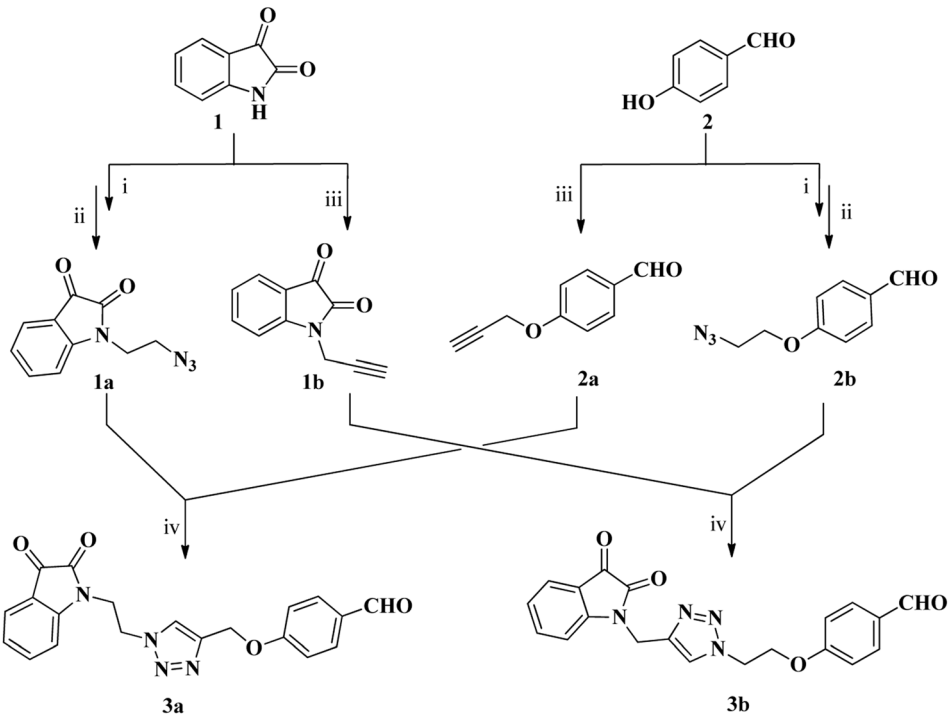

Scheme 1 Synthesis of isatin–triazole hybrids **3a** and **3b**; reagents and conditions: (i) dibromoethane (2.1 eq.), DMF, K_2CO_3 (ii) NaN_3 (1.2 eq.), DMF(iii) propargyl bromide, DMF, K_2CO_3 (iv) $CuSO_4 \cdot 5H_2O$, sodium ascorbate, EtOH : H_2O (9 : 1), rt.

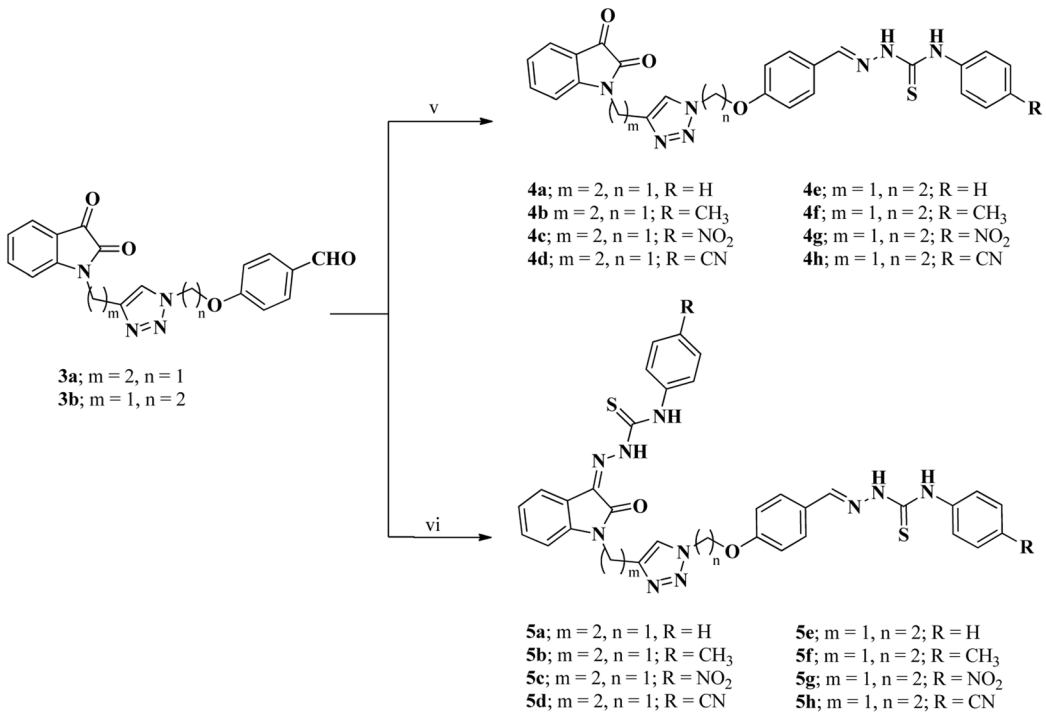

Scheme 2 Synthesis of mono and bis-thiosemicarbazones (**4a–h** and **5a–h**) of isatin–triazole hybrids (**3a** and **3b**); reagents and conditions: (v) N^4-substituted thiosemicarbazides (1.1 eq.), EtOH, rt; (vi) N^4-substituted thiosemicarbazides (2.1 eq.), EtOH, CH_3COOH (cat.), reflux.

isatin and triazole, respectively and a singlet present downfield at 5.25 ppm for oxymethylene present next to triazole further support its formation. Similarly, two triplets for two methylene protons attached to triazole and phenoxy ring respectively appeared at 4.45 ppm and 4.80 ppm and a singlet for the methylene that links isatin and triazole appeared downfield at

5.05 ppm supports the formation of **3b**. Finally, the presence of singlet at 9.91 ppm and 9.88 ppm, respectively for one proton integration corresponding to aldehyde proton of **3a** & **3b**, respectively confirms their formation. The ^{13}C NMR spectrum showed two characteristic signals one at 124.4 ppm and 124.0 ppm respectively and a relatively less intense signal at 142.9 ppm and 141.9 ppm respectively due to C-5 and C-4 of triazole ring further confirms the formation of 1,4-disubstituted triazole ring in **3a** & **3b**. Moreover, three signals at (40.3 ppm, 47.4 ppm, 61.6 ppm) and (35.3 ppm, 49.7 ppm, 66.3 ppm), respectively due to two carbons of ethyl linker and one carbon of –OCH_2 group also indicated the formation of desired products. The presence of carbonyl carbons of aldehyde and ketone at 182.9–190.6 ppm provided the final evidence for the formation of intermediates **3a** & **3b**. Finally, the peak at *m*/*z* 412 $[M + 36]^-$ for $C_{20}H_{16}O_4N_4$ in the LCMS spectrum also support the proposed structures of **3a** & **3b**.

Similarly, the presence of two signals for NH protons at 11.68 ppm and 9.98 ppm and a singlet at 8.25 ppm for the azomethine proton in ^{1}H NMR spectrum of representative mono-thiosemicarbazone **4f** clearly suggests the selective and successful condensation of thiosemicarbazide at aldehydic position. Moreover, a singlet at 2.30 ppm for methyl protons further confirms the formation of **4f**. In contrast to the ^{1}H NMR spectrum of **4f**, the bis-thiosemicarbazone **5e** shows four signals for NH protons at 12.76 ppm, 11.73 ppm, 10.89 ppm and 10.05 ppm and a singlet of azomethine proton at 8.27 ppm. In the ^{13}C NMR spectrum, an upfield signal of **4f** appeared at 142.9 ppm and two signals of **5e** observed at 143.8 ppm and 142.9 ppm corresponding to imine moieties of thiosemicarbazones strongly support the formation of mono- and bis-thiosemicarbazones **4f** and **5e** respectively. The absence of signal for aldehydic carbonyl and both aldehyde and ketone carbonyls observed in the respective starting materials and the appearance of signal for thiocarbonyl at 176.2 ppm and two signals at 176.8 and 176.1 ppm for **4f** and **5e** respectively also support the formation of desired thiosemicarbazones. The final evidence for the formation of mono- and bis-thiosemicarbazones was obtained from their LCMS data. The observation of peaks at 539 *m*/*z* and 673 *m*/*z* respectively corresponding to $[M]^-$ clearly confirms the formation of **4f** and **5e**. All the other compounds of the series are characterized in a similar manner (see Experimental section for more details).

2.3 Computational study

2.3.1 DFT studies. Obtaining the structural parameters from the optimized geometry of the synthesized molecules that lead to the information of molecular interactions is considered as preliminary step before molecular docking analyses.[22] In this context, the Density Functional Theory (DFT) calculations, specifically the 6-311G (d,p) basis set at the B3LYP level were carried out.[57–59]

The highest occupied molecular orbital (HOMO) and the lowest unoccupied molecular orbital (LUMO) are two popular quantum chemical parameters.[60] The energies of these molecular orbitals, also known as frontier molecular orbitals (FMOs), are important parameters for predicting the reactivity of a chemical species.[61] These parameters are critical in molecular reactivity, because HOMO (highest energy orbital with electrons) can act as an electron donor, while LUMO orbital serves as an electron acceptor because it has a lower energy than the other orbitals and can accept electrons.[62,63] The energies of the HOMO and LUMO orbital values are shown in Table 1. Higher E_{HOMO} value of compound **3b** indicated the greater tendency for electron donation to a suitable acceptor molecule with a low energy and empty molecular orbital.[64] Negative E_{HOMO} and E_{LUMO} values, on the other hand, indicated the stability of the compounds under investigation.[65,66] Quantum mechanical calculations[67] (Table 2) have been used to investigate the properties of donors and acceptors in molecules. The LUMO–HOMO energy differences were measured, demonstrating that the energy gap represents the chemical behavior of a molecule.[68] The $E_{LUMO–HOMO}$ energy gap separation was used to assess the kinetic stability of the compounds.[69] Frontier molecular orbital energies along with the energy gap between HOMO and LUMO of compounds (**3a–b**, **4a–h** and **5a–h**) is given in Table 1.

FMOs are studied in order to investigate the bioactivity and catalytic behavior of the compounds.[17,70] According to FMO theory, both HOMO and LUMO are important factors in understanding electronic transitions, molecular reactivities, and intermolecular interactions, and thus provide insight into bioactivity.[71–73] Furthermore, the presence of FMOs on the same side of the molecule significantly reduces biological activity.[74] The distribution patterns of FMOs (HOMOs and LUMOs) of synthesized triazole hybrids at ground states are shown in Fig. 2. The green color represents a low electron density while the red represents the high electron density.[75] The addition of substituents to benzene ring has little effect on the pi-electron cloud of HOMO and LUMO. Interestingly, the energy gap ($E_{LUMO–HOMO}$) values of the synthesized derivatives of hybrid **3b**

Table 1 FMO energy of isatin triazole hybrids (**3a** and **3b**) and their thiosemicarbazones (**4a–h** and **5a–h**)

S. No.	Compound (R)	E_{LUMO} (eV)	E_{HOMO} (eV)	ΔE (eV)
1	**3a**	0.73	−1.57	2.31
2	**3b**	0.95	−1.22	2.18
3	**4a** (H)	0.76	−4.91	5.68
4	**4b** (CH_3)	0.78	−4.87	5.66
5	**4c** (NO_2)	−0.36	−0.51	0.14
6	**4d** (CN)	0.52	−5.21	5.74
7	**4e** (H)	0.72	−3.05	3.78
8	**4f** (CH_3)	0.82	−3.04	3.86
9	**4g** (NO_2)	−0.24	−0.33	0.09
10	**4h** (CN)	0.09	−3.12	3.21
11	**5a** (H)	0.84	−5.01	5.85
12	**5b** (CH_3)	0.48	−4.80	5.28
13	**5c** (NO_2)	−1.76	−3.58	1.82
14	**5d** (CN)	0.68	−5.65	6.34
15	**5e** (H)	0.71	−3.11	3.82
16	**5f** (CH_3)	0.84	−3.18	4.02
17	**5g** (NO_2)	−0.03	−3.64	3.61
18	**5h** (CN)	0.05	−3.28	3.34

Table 2 Reactivity indices of isatin triazole hybrids (**3a** and **3b**) and their mono and bis-thiosemicarbazones (**4a–h** and **5a–h**)

S. No.	Compound	EA[a]	IP[b]	χ^c	η^d	S^e	μ^f	ω^g
1	**3a**	−0.73	1.57	0.42	1.15	0.43	−0.42	−0.07
2	**3b**	−0.95	1.22	0.13	1.09	0.45	−0.13	0.07
3	**4a**	−0.76	4.91	2.07	2.84	0.17	−2.07	0.75
4	**4b**	−0.78	4.87	2.04	2.83	0.17	−2.04	0.73
5	**4c**	0.36	0.51	0.43	0.08	6.25	−0.43	1.15
6	**4d**	−0.52	5.21	2.34	2.87	0.17	−2.34	0.95
7	**4e**	−0.72	3.05	1.16	1.89	0.26	−1.16	0.35
8	**4f**	−0.82	3.04	1.11	1.93	0.25	−1.11	0.31
9	**4g**	0.24	0.33	0.28	0.04	12.5	−0.28	0.98
10	**4h**	−0.09	3.12	1.51	1.61	0.31	−1.51	0.70
11	**5a**	−0.84	5.01	2.08	2.92	0.17	−2.08	0.74
12	**5b**	−0.48	4.80	2.15	2.64	0.18	−2.15	0.87
13	**5c**	1.76	3.58	2.67	0.91	0.54	−2.67	3.91
14	**5d**	−0.68	5.65	2.48	3.17	0.15	−2.48	0.97
15	**5e**	−0.71	3.12	1.20	1.91	0.26	−1.20	0.37
16	**5f**	−0.84	3.18	1.17	2.01	0.24	−1.17	0.34
17	**5g**	0.03	3.64	1.83	1.80	0.27	−1.83	0.93
18	**5h**	−0.05	3.28	1.61	1.67	0.29	−1.61	0.77

[a] Electron affinity. [b] Ionization Energy. [c] Electronegativity. [d] Chemical hardness. [e] Chemical softness. [f] Chemical potential. [g] Electrophilicity.

differ only slightly, with all derivatives falling within the range of 0.09–4.02 eV while those for hybrid **3a** derivatives lies in the range of 0.14–6.34 eV. Results showed that incorporating nitro substituents on the phenyl ring lowers the energy separation gap ($E_{LUMO-HOMO}$). In fact, nitro compounds **4c**, **4g** and **5c** (0.14, 0.09, 1.82 eV, respectively) are found to be the lowest among all the synthesized derivatives (see Table 1). The lower $E_{LUMO-HOMO}$ corresponds to the greater the biological potential,[17] by increasing the chemical reactivity and catalytic activity of these synthesized hybrids. Recent studies indicated that molecules with an FMO energy gap of less than 2.5 eV are more likely to bind to specific protein targets.[76] Herein, compounds **3b**, **4c**, **4g** and **5c** displayed the FMO energy gap of less than 2.2 eV as shown in Fig. 2, hence expected to show the best binding interactions with the biological targets.

Beside the evaluation of quantum chemical parameters[77] *i.e.* frontier molecular orbitals and separation energies ΔE_{gap}; global reactivity descriptors[78] such as ionization potentials ($IP = -E_{HOMO}$), electron affinity ($EA = -E_{LUMO}$), electronegativities [$\chi = (IP + EA)/2$], chemical potentials ($\mu = -\chi$), chemical hardness [$\eta = (IP - EA)/2$], chemical softness ($S = 1/2\eta$), global electrophilicity or electrophilicity index ($\omega = \mu^2/2\eta$) have also been calculated.[79–82] Chemical descriptors are used to analyze drug properties and interactions with biological targets.[83–85] Results showed that chemically harder and more stable molecules have a larger LUMO–HOMO energy gap than softer and less stable molecules.[62] It was also observed that chemically reactive molecules showed greater chemical potential.[86] The lower LUMO value corresponds to the higher electron acceptance ability,[87] and the compound **5c** showed the highest electron affinity value among the series (Table 2). Similarly, the higher HOMO value corresponds to the higher electron donor ability,[88] and the compound **4g** displayed the least value of ionization potential, thus indicating the highest electron donor ability of the compound among the synthesized derivatives (Table 2).

Electronegativity refers to a ligand's ability to bind to a protein, which is important for successful binding.[89] A direct relationship was observed between electronegativity values (χ) values and tendency to accept electrons *i.e.* electron affinity (Table 2). Results showed that compound **5c** (bisthiosemicarbazone having two nitro substituents) (Table 2) displayed the highest electronegativity value, thus making it more susceptible to accept electrons, through the electron withdrawing effect, hence showing its higher catalytic ability and binding affinity with the target protein.[90–92]

The electrophilicity index (ω) indicates the compound's ability to interact with electron-rich sites of biological targets and measures the tendency to accept electrons from the environment.[93] The most stable compound is the one with a low

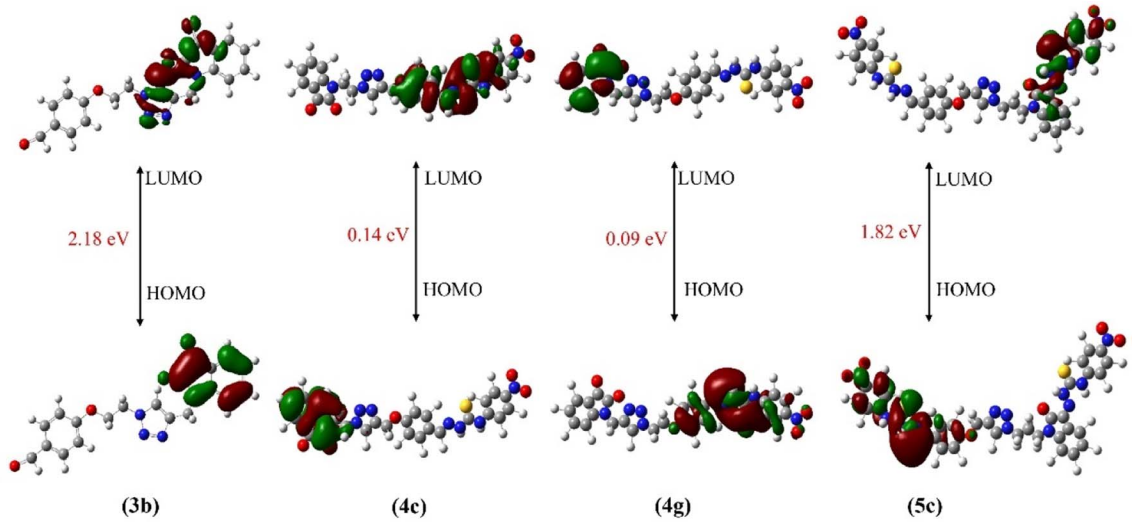

Fig. 2 HOMO and LUMO of **3b**, **4c**, **4g** and **5c**.

electrophilicity value *i.e.* **3a** among the studied substrates (Table 2). As we moved from electron donating to electron withdrawing substituents in the substrate, the electrophilicity index value increased. Compound **5c** having the *p*-nitro substituent displayed the highest electrophilicity index value and is found to the most reactive among the series (Table 2), thus showed greater potential to bind with the biological target. Compounds with a higher electrophilicity index value are more reactive and less stable, whereas compounds with a lower electrophilicity index value are more stable and less reactive.[94] Furthermore, lower chemical potential (μ) value makes a substituent more electrophilic (electron-seeking), and in this case, the value for the compound **5c** having the p-nitro substituent is the lowest *i.e.* −2.67 eV among the series (Table 2).

Hardness refers to a resistance of compound to electron donation or acceptance and plays an important role in water solubility.[89] Overall range of global hardness (η) was found to be 0.04–0.17 eV while the hardest character was shown by the compound **5d** within the series (Tabe 2). Softness, the inverse of hardness, refers to a compound's ability to donate or accept electrons, as well as their reactivity with biological targets.[95] Considering the soft nature of the synthesized compounds, the compound **4g** having nitro substituent showed the highest value of chemical softness (S) (Table 2). Compound **4g** being the most reactive compound among the series (Table 2), appeared as a favorable candidate for efficient applications in different synthetic routes and further theoretical calculations, possibly due to the extended conjugation and electron withdrawing nature of nitro group. Moreover, the lowest hardness (η) and the highest softness (S) value of compound **4g** (Table 2) indicate that it is less likely to undergo rapid structural changes during binding, which is crucial for stable protein interactions. Concludingly, the DFT studies provided comprehensive analysis of theoretical structure stability and mechanistic explanations of chemical properties of the synthesized compounds for their ability to interact with biological targets.

2.3.2 Molecular docking studies. Molecular docking provides a theoretical direction for visual representation of the binding characteristics of the ligand molecule to the protein under study, as well as guidelines for further exploration and validation of experimental data.[96,97] It is a convenient predictive tool in drug discovery which assess in computer-aided drug designing.[98] The molecular docking study was carried out using the AutoDock Vina software package,[99] for the selected compounds **3b**, **4c**, **4g** and **5c** having ΔE_{gap} less than 2.2 eV as indicated by the DFT results based on the optimised structures of the synthesized thiosemicarbazones of isatin–triazole hybrids.

PASS online (prediction of activity of spectra for substances)[100] predicted the profound anticancer potential of synthesized thiosemicarbazones of isatin triazole hybrids. Phosphoinositide 3-kinase PI3K protein was chosen for this study because of its well-known roles in regulating cell growth and survival, particularly in cancer.[89,101] The selected active site of the PI3K inhibitor of PDB ID (4TV3)[102,103] was downloaded from RCSB[104] protein data bank. The structure of desired PI3K protein was prepared for docking using AutoDock Tools.[105,106]

The primary goal of the molecular docking studies was to evaluate the binding potential of the synthesized compounds as well as molecular interaction with various amino acid residues of the membrane protein PI3K. The Autodock Vina 1.5.7 (ref. 99) was used to obtain docking simulations and the visualization of protein-ligand complex was performed using the Discovery Studio.[107] The most stable anchoring conformations having the lowest binding energy values, as well as interacting residues were visualized through three-dimensional and two-dimensional models, as depicted in Fig. 3, which were created using the Discovery Studio Visualizer.[108] It has been demonstrated that receptors have active sites that are capable to behave both as hydrogen bond donor and acceptor as well.[75]

The 2D representation in Fig. 3 helps to clearly visualize the types of interactions including hydrophobic interactions, hydrogen bonding, donor atoms, acceptor atoms, and π–π stacking interactions between the studied compounds and the cancer protein's active sites. Table 3 shows the binding energy of enzymes on the ligand, hydrostatic interactions, and hydrogen bonding in the selective host–guest systems. Results displayed the following decreasing order of binding affinity score for the studied compounds **5c** > **4g** > **4c** > **3b** (Table 3).

Among the selected compounds, the compound **5c** having two nitro substituents displayed the highest binding energy score of −10.3 kcal mol^{-1}. The amino His 670(A), Met 811(A), Ile 633(A), Leu 632(A), Cys 838(A) formed hydrogen bonding with the nitrogen of –NH of thiosemicarbazones and oxygen of nitro substituents in compound **5c** (Fig. 3). Moreover, carbon–hydrogen bond formation was observed with Gly 837(A) and the amino acids Glu 172(A), Glu 821(A) showed π-sulphur and π-anion interactions with the ligand and the amino acid Phe 666(A) formed π-alkyl and π–π stacking interactions with the benzene ring. Similarly, the compound **4g** which is 4-nitro substituted mono-thiosemicarbazone derivative of isatin triazole hybrid **3b** displayed the second best binding score of −8.9 kcal mol^{-1}, alongwith several binding interactions such as hydrogen bonding of carbonyl oxygen of isatin, nitrogen of 1,2,3-triazole and –NH of thiosemicarbazone moiety with the Lys 548(A), Asn 575(A), Tyr 361(A) residues respectively (Table 3). Furthermore, carbon hydrogen bond, π-alkyl and salt bridge interactions with the active site residues of PI3K protein were also depicted in 2D model (Fig. 3) of compound **4g**.

The docking scores suggested that isatin–triazole hybrid **3b** posses lesser binding affinity with target protein, as compared to its 4-nitro substituted mono-thiosemicarbone derivative **4g**. While the 4-nitro substituted bis-thiosemicarbone derivative **5c** displayed even superior binding affinity with the target protein. These results reveal the importance of substitution on benzene ring and presence of thiosemicarzaone scaffold on the isatin–triazole hybrid for enhanced binding interaction of the drug molecules which is also supported by the literature.[22,109] Molecular docking results are in good agreement with the findings of DFT analyses and these computational explanations suggested that the synthesized thiosemicarbazones of isatin–triazole hybrids may act against PI3K as anti-cancer agents.

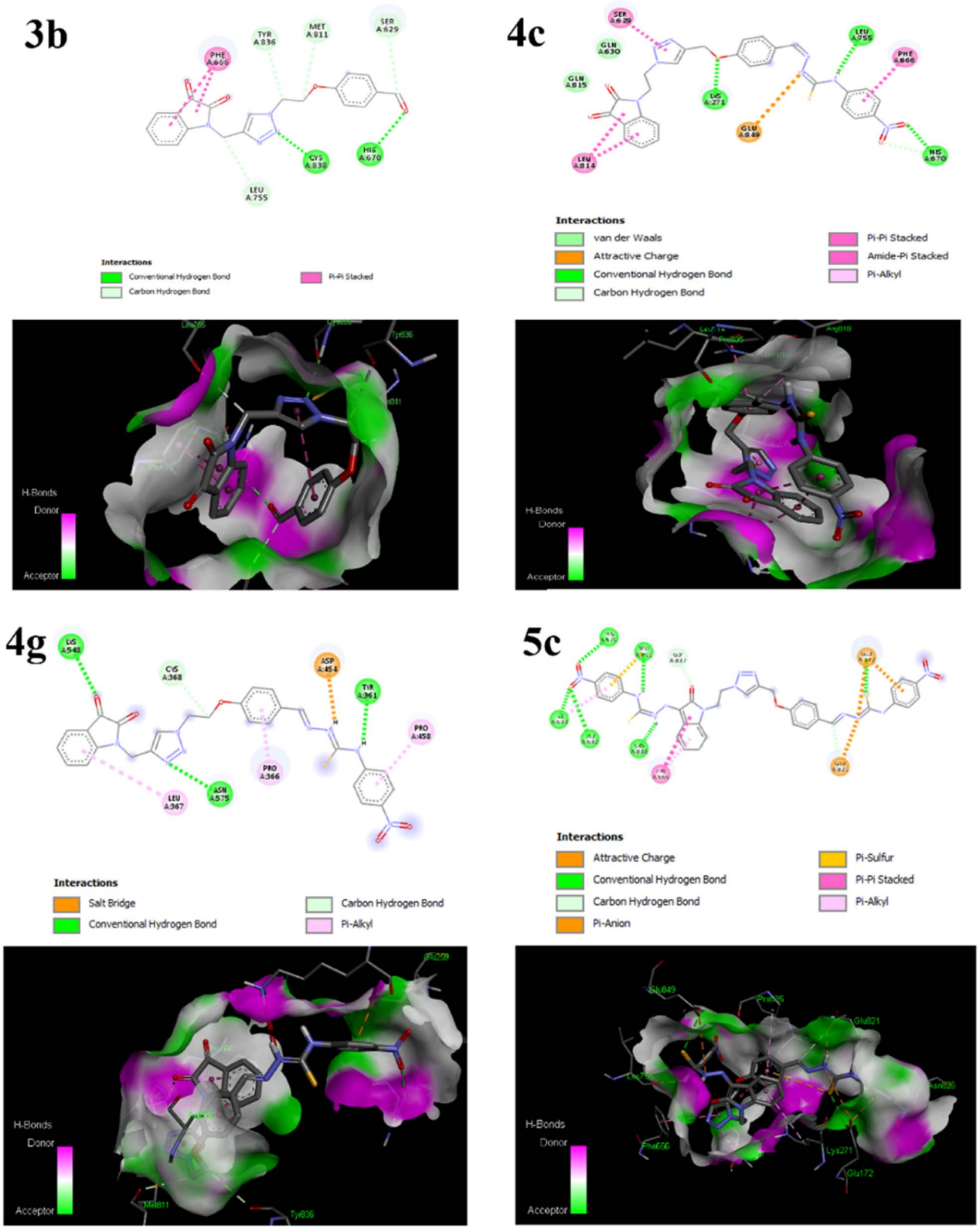

Fig. 3 Diagrammatic representation of molecular interactions of the ligand molecules (**3b**, **4c**, **4g** and **5c**) with various amino acid residues in the binding pocket of the protein PI3K.

Table 3 The interaction analysis of the PI3K protein on the basis of molecular docking studies with the mono and bis-thiosemicarbazones of isatin–triazole hybrids

S. No.	Drug name (ligand)	Binding energy (kcal mol^{-1})	Hydrogen bond interaction	Hydrostatic interaction with amino acids
1	**3b**	−8.3	Cys 838(A), His 670(A), Ser 629(A), Met 811(A), Tyr 836(A)	Leu 755(A), Phe 666(A)
2	**4c**	−8.6	Gln 630 (A), Gln 815 (A), Lys 271 (A), Leu 755 (A), His 670 (A)	Phe 666(A), Leu 814(A), Glu 849 (A), Ser 629 (A)
3	**4g**	−8.9	Lys 548(A), Asn 575(A), Tyr 361(A)	Leu 367(A), Cys 368(A), Pro 366(A), Asp 454(A), Pro 458(A)
4	**5c**	−10.3	His 670(A), Met 811(A), Ile 633(A), Leu 632(A), Cys 838(A)	Phe 666(A), Gly 837(A), Glu 172(A), Glu 821(A)

3. Conclusions

A series of mono- and bis-thiosemicarbazones have been synthesized starting from two novel isatin–triazole hybrid intermediates, in turn obtained through the Cu(I)-sodium ascorbate catalysed click reaction, in excellent yield. All the synthesized compounds are characterized by their spectral (FT-IR, ^{1}H & ^{13}C NMR, LCMS) and analytical data. The DFT studies carried out on these compounds showed that the compound **5c** (4-nitro-substituted bis-thiosemicarbazone) exhibited the highest electron affinity, electronegativity and electrophilicity index values among the series, hence exhibiting the greater potential to bind with the target protein. The outcome of DFT studies was further validated by molecular docking analysis against the active sites of the phosphoinositide 3-kinases (PI3Ks), indicating the potential of compound **5c** (block the active site of targeted enzyme with the lowest binding score of −10.3 kcal mol^{-1}) to be studied as an anticancer agent.

4. Experimental

4.1 Chemicals and materials

The used chemicals and materials were supplied as ESI.†

4.2 Computational details

The molecular structure of all the synthesized compounds were optimized using Gaussian 09 Package.[110] The optimized structures were used to calculate the electronic properties of the synthesized compounds. The frontier molecular orbitals HOMO and LUMO alongwith other descriptors were calculated using Gauss View to understand the effect of substituents on the reactivity of compounds. For molecular docking studies the Autodock Vina 1.5.7 (ref. 99) was used for docking simulations, and the Discovery Studio[107] was used for visualization.

4.3 Synthesis of 4-((1-(2-(2,3-dioxoindolin-1-yl)ethyl)-1*H*-1,2,3-triazol-4-yl)-methoxy)benzaldehyde (3a)

For the synthesis of **3a**, the reported conditions[55] of the click reaction were employed. In a stirred solution of the 1-(2-azidoethyl)isatin **1a** (0.10 g, 0.46 mmol) and 4-(prop-2-ynyloxy) benzaldehyde **2a** (0.07 g, 0.46 mmol) in 10 mL ethanol : water (9 : 1), addition of copper sulphate (0.00625 g, 0.025 mmol) was followed by sodium ascorbate (0.013 g, 0.066 mmol) addition at room temperature. Upon the completion of the reaction, as indicated by the TLC (*n*-hexane: EtOAc, 1 : 1), ice-cold water was added to the reaction mixture and the precipitates formed were filtered out and dried. Recrystallization from ethanol was performed to obtain the purified product.

Appearance: bright orange solid; yield: 89%; melting point: 157–160 °C; R_f: 0.53 (*n*-hexane: EtOAc, 1 : 1); FT-IR $\bar{\nu}$ (cm^{-1}): 3129, 3049 (C_{sp^2}–H stretch), 2928, 2873 (C_{sp^3}–H stretch), 2823, 2724 (C_{sp^2}–H stretch, aldehyde), 1731 (C=O stretch, ketone), 1692 (C=O stretch, aldehyde), 1598 (C=O stretch, lactam), 1509 (C=C stretch, aromatic ring), 1471 (C_{sp^3}–H bend, methylene), 1258 (C_{sp^2}–O stretch, ether), 1217 (C–N stretch, lactam), 1160 (C_{sp^3}–O stretch, ether), 810 (C–H bend, 1,4-disubstitution),

754 (C–H bend, 1,2-disubstitution); ^{1}H NMR (300 MHz, $CDCl_3$) δ (ppm): 9.91 (s, 1*H*, –CHO), 8.25 (s, 1*H*, triazole-H), 7.88 (d, ^3J = 8.7 Hz, 2*H*, Ar–H), 7.52 (d, ^3J = 7.3 Hz, 1*H*, Ar–H), 7.43 (t, ^3J = 7.5 Hz, 1*H*, Ar–H), 7.10–7.04 (t, 1*H*, ^3J = 7.3 Hz, Ar–H), 7.06–7.03 (d, 2*H*, ^3J = 8.7 Hz, Ar–H), 6.84 (d, ^3J = 7.9 Hz, 1*H*, Ar–H), 5.25 (s, 2*H*, –OCH_2), 4.84 (t, ^3J = 6 Hz, 2*H*, –CH_2-triazole),4.30 (t, ^3J = 6 Hz, 2*H*, –CH_2-isatin); ^{13}C NMR (75 MHz, $CDCl_3$) δ (ppm): 190.3 (C=O aldehyde), 182.9 (C=O ketone), 163.3, 158.1(C=O lactum), 150.6, 142.9 (C-5 triazole), 138.1, 131.6, 130.4, 125.0, 124.4 (C-4 triazole), 123.4, 117.6, 115.1, 109.9, 61.6 (–CH_2 phenoxy), 47.4 (–CH_2 triazole), 40.3 (–CH_2 isatin); LC-MS *m*/*z* 412 [M + 36]; anal. calcd for $C_{20}H_{16}N_4O_4$: C, 63.83; H, 4.29; N, 14.89; O, 17.00; found: C, 63.98; H, 4.15; N, 14.93.

4.4 Synthesis of 4-(2-(4-((2,3-dioxoindolin-1-yl)methyl)-1*H*-1,2,3-trizol-1-yl)-ethoxy)-benzaldehyde (3b)

For the synthesis of **3b**, reported reaction conditions for click reaction were utilized. Copper sulphate (0.04 g, 0.16 mmol) and sodium ascorbate (0.08 g, 0.23 mmol) were added in succession, to the stirred solution of previously synthesized 1-(prop-2-ynyl) indoline-2,3-dione **1b** (0.20 g, 1.08 mmol) and 4-(2-azidoethoxy)benzaldehyde **2b** (0.21 g, 1.08 mmol) in 10 mL ethanol: water (9 : 1) at room temperature. Progress of reaction was monitored by TLC (*n*-hexane: EtOAc, 1 : 1).After the reaction completion, ice cold water (15 mL) was added to the reaction mixture and the precipitates formed were filtered off, dried and recrystallized from ethanol to obtain the pure product.

Appearance: orange solid; yield: 85%; melting point: 168–170 °C; R_f: 0.52 (*n*-hexane: EtOAc, 1 : 1); FT-IR $\bar{\nu}$ (cm^{-1}): 3141, 3031 (C_{sp^2}–H stretch), 2970, 2942 (C_{sp^3}–H stretch), 2847, 2759 (C_{sp^2}–H stretch, aldehyde), 1728 (C=O stretch, ketone), 1673 (C=O stretch, aldehyde), 1600 (C=O stretch, lactam), 1508 (C=C stretch, aromatic), 1469 (C_{sp^3}–H bend, methylene), 1244 (C_{sp^2}–O stretch, ether), 1213 (C–N stretch, lactam), 1159 (C_{sp^3}–O stretch, ether), 831 (C–H bend, 1,4-disubstitution), 755 (C–H bend, 1,2-disubstitution); ^{1}H NMR (300 MHz, $CDCl_3$) δ (ppm): 9.88 (s, 1H, –CHO) 7.85 (s, 1*H*, triazole-H) 7.81 (d, ^3J = 7.5 Hz, 2*H*, Ar–H), 7.57 (m, 2*H*, Ar–H), 7.31 (d, ^3J = 8.1 Hz, 2*H*, Ar–H), 7.11 (t, ^3J = 7.5 Hz, 1*H*, Ar–H), 6.95 (d, ^3J = 8.7 Hz, 2H, Ar–H), 5.03 (s, 2H, –CH_2-isatin), 4.80(t, ^3J = 4.2 Hz, 2H, –CH_2-trizaole), 4.45 (t, ^3J = 4.2 Hz, 2*H*, –OCH_2); ^{13}C NMR (75 MHz, $CDCl_3$) δ (ppm): 190.6 (C=O aldehyde), 183.0 (C=O ketone), 162.4, 157.9 (C=O lactum), 150.1, 141.9 (C-5 triazole), 138.6, 132.0, 130.7, 125.3, 124.2 (C-4 triazole), 124.0, 117.5, 114.7, 111.4, 66.3 (–CH_2 phenoxy), 49.7 (–CH_2 triazole), 35.3 (–CH_2 isatin); LC-MS *m*/*z* 412 [M + 36]; anal. calcd for $C_{20}H_{16}N_4O_4$: C, 63.83; H, 4.29; N, 14.89; O, 17.00; found: C, 63.92; H, 4.41; N, 14.74.

4.5 General procedure for the synthesis of isatin–triazole derived mono-thiosemicarbazones (4a–h)

For the synthesis of mono-thiosemicarbazones **4a–h** of two different types of isatin–triazole hybrids **3a** and **3b**, same procedure was followed. To the stirred ethanolic solution of isatin–triazole hybrid (0.1 g, 0.27 mmol), suitable N^4-substituted thiosemicarbazide **3c** (1.1 eq., 0.30 mmol) was added under vigorous stirring. The reaction was carried out at room temperature for 6 hours and progress of reaction was monitored after regular intervals by TLC (*n*-hexane: ethyl acetate 7 : 3). The precipitates formed upon completion, were filtered, washed, dried and recrystallized when required to obtain the pure product.

By following the above procedure, a series of mono-thiosemicarbazone derivatives **4a–h** having different thiosemicarbazide moieties were synthesized.

4.5.1 1-((4-((1-(2-(2,3-Dioxoindolin-1-yl)ethyl)-1*H*-1,2,3-triazol-4-yl)methoxy) phenyl)methylene)-4-phenylthiosemicarbazide (4a). Appearance: orange-yellow solid; yield: 75%; melting point: 215–218 °C; R_f: 0.52 (*n*-hexane: EtOAc, 4 : 6); FT-IR $\bar{\nu}$ (cm^{-1}):3300 (N–H stretch), 3129, 3049 (C_{sp^2}–H stretch), 2928, 2873 (C_{sp^3}–H stretch), 1737 (C=O stretch, ketone), 1600 (C=O stretch, lactam), 1525 (C=N stretch, imine),1508 (C=C stretch, aromatic ring), 1467 (C_{sp^3}–H bend, methylene), 1274 (C_{sp^2}–O stretch, ether), 1201 (C–N stretch, lactam), 1165 (C_{sp^3}–O stretch, ether), 833 (C–H bend, 1,4-disubstitution), 755 (C–H bend, 1,2-disubstitution); ^{1}H NMR (300 MHz, DMSO-d_6) δ (ppm): 11.82 (s, 1*H*, –NH), 9.98 (s, 1*H*, –NH), 8.38 (s, 1*H*, –CH=N), 7.36 (s, 1*H*, –CH triazole), 8.37–6.89 (m, 13*H*, Ar–H), 5.13 (s, 2*H*, –CH_2 isatin), 4.71 (t, 2*H*, ^3J = 6 Hz, –OCH_2), 4.14 (t, 2*H*, ^3J = 6 Hz, –CH_2 triazole); ^{13}C NMR (75 MHz, DMSO-d_6) δ (ppm): 183.4, 161.8 (C=S), 160.2, 158.6, 150.6, 149.6, 142.9 (C=N azomethine), 139.7, 138.6, 129.6, 129.4, 127.3, 125.9, 124.9, 124.1, 123.7, 117.8, 115.5, 110.7, 61.6, 47.4, 35.4; LC-MS *m*/*z* 525 [M^-]; anal. calcd for $C_{27}H_{23}N_7O_3S$: C, 61.70; H, 4.41; N, 18.66; found: C, 61.63; H, 4.29; N, 18.77.

4.5.2 1-((4-((1-(2-(2,3-Dioxoindolin-1-yl)ethyl)-1*H*-1,2,3-triazol-4-yl)methoxy) phenyl)methylene)-4-*p*-tolylthiosemicarbazide (4b). Appearance: yellow solid; yield: 79%; melting point: 196–198 °C; R_f: 0.46 (*n*-hexane: EtOAc, 4 : 6); FT-IR $\bar{\nu}$ (cm^{-1}):3300 (N–H stretch), 3129, 3049 (C_{sp^2}–H stretch), 2928, 2873 (C_{sp^3}–H stretch), 1731 (C=O stretch, ketone), 1612 (C=O stretch, lactam), 1541 (C=N stretch, imine),1506 (C=C stretch, aromatic ring), 1469 (C_{sp^3}–H bend, methylene), 1271 (C_{sp^2}–O stretch, ether), 1214 (C–N stretch, lactam), 1170 (C_{sp^3}–O stretch, ether), 815 (C–H bend, 1,4-disubstitution), 756 (C–H bend, 1,2-disubstitution); ^{1}H NMR (300 MHz, DMSO-d_6) δ (ppm): 11.68 (s, 1*H*, –NH), 9.98 (s, 1*H*, –NH), 8.25 (s, 1*H*, –CH=N), 8.07 (s, 1*H*, –CH triazole), 7.81–6.89 (m, 12*H*, Ar–H), 4.97 (s, 2*H*, –CH_2 isatin), 4.74 (t, 2*H*, ^3J = 6 Hz, –OCH_2), 4.42 (t, 2*H*, ^3J = 6 Hz, –CH_2 triazole), 2.31 (s, 3*H*, –CH_3); ^{13}C NMR (75 MHz, DMSO-d_6) δ (ppm): 183.5, 176.2 (C=S), 159.7, 158.2, 150.6, 142.9 (C=N azomethine), 141.9, 138.5, 137.0, 134.8, 129.7, 129.3, 128.9, 127.5, 126.3, 124.9, 124.7, 123.8, 118.0, 115.4, 115.1, 111.6, 66.6, 49.5, 35.4, 21.0 (CH_3); LC-MS *m*/*z* 539 [M^-]; anal. calcd for $C_{20}H_{16}N_4O_4$: C, 63.83; H, 4.29; N, 14.89; found: C, 63.88; H, 4.17; N, 14.96.

4.5.3 1-((4-((1-(2-(2,3-Dioxoindolin-1-yl)ethyl)-1*H*-1,2,3-triazol-4-yl)methoxy) phenyl)methylene)-4-(4-nitrophenyl) thiosemicarbazide (4c). Appearance: yellow solid; yield: 76%; melting point: 220–221 °C; R_f: 0.43 (*n*-hexane: EtOAc, 4 : 6); FT-IR $\bar{\nu}$ (cm^{-1}):3300 (N–H stretch), 3129, 3049 (C_{sp^2}–H stretch), 2928, 2873 (C_{sp^3}–H stretch), 1732 (C=O stretch, ketone), 1683 (C=O stretch, lactam), 1600 (C=N stretch, imine), 1543 (N–O stretch, asymmetric, nitro), 1506 (C=C stretch, aromatic ring),

1465 (C_{sp^3}–H bend, methylene), 1328 (N–O stretch, symmetric, nitro), 1249 (C_{sp^2}–O stretch, ether), 1203 (C–N stretch, lactam), 1166 (C_{sp^3}–O stretch, ether), 831 (C–H bend, 1,4-disubstitution), 758 (C–H bend, 1,2-disubstitution); ^{1}H NMR (300 MHz, DMSO-d_6) δ (ppm): 12.03 (s, 1*H*, –NH), 9.98 (s, 1*H*, –NH), 8.42–6.87 (m, 15*H*, CH=N, –CH triazole, Ar–H), 5.15 (s, 2*H*, –CH_2 isatin), 4.68 (t, 2*H*, ^3J = 6 Hz, –OCH_2), 4.14 (t, 2*H*, ^3J = 6 Hz, –CH_2 triazole); ^{13}C NMR (75 MHz, DMSO-d_6) δ (ppm): 183.4, 161.7 (C=S), 160.2, 158.6, 150.6, 149.6, 142.9 (C=N azomethine), 139.6, 138.6, 129.6, 129.4, 127.4, 125.9, 124.9, 124.1, 123.7, 117.8, 115.5, 110.6, 61.6, 47.4, 35.4; LC-MS *m*/*z* 570 [M^-]; anal. calcd for $C_{27}H_{22}N_8O_5S$: C, 56.84; H, 3.89; N, 19.64; found: C, 56.78; H, 3.69; N, 19.47.

4.5.4 4-(4-Cyanophenyl)-1-((4-((1-(2-(2,3-dioxoindolin-1-yl) ethyl)-1*H*-1,2,3-triazol-4-yl)methoxy)phenyl)methylene) thiosemicarbazide (4d). Appearance: bright yellow solid; yield: 82%; melting point: 236–238 °C; R_f: 0.41 (*n*-hexane: EtOAc, 4 : 6); FT-IR $\bar{\nu}$ (cm^{-1}):3300 (N–H stretch), 3129, 3049 (C_{sp^2}–H stretch), 2928, 2873 (C_{sp^3}–H stretch), 2250 (C≡N stretch, cyano) 1735 (C=O stretch, ketone), 1606 (C=O stretch, lactam), 1537 (C=N stretch, imine),1510 (C=C stretch, aromatic ring), 1467 (C_{sp^3}–H bend, methylene), 1249 (C_{sp^2}–O stretch, ether), 1195 (C–N stretch, lactam), 1169 (C_{sp^3}–O stretch, ether), 837 (C–H bend, 1,4-disubstitution), 752 (C–H bend, 1,2-disubstitution); ^{1}H NMR (300 MHz, DMSO-d_6) δ (ppm): 11.68 (s, 1*H*, –NH), 9.99 (s, 1*H*, –NH), 8.29–6.89 (m, 14*H*, –CH=N, –CH triazole Ar–H), 4.97 (s, 2*H*, –CH_2 isatin), 4.74 (t, 2*H*, ^3J = 6 Hz, –OCH_2), 4.42 (t, 2*H*, ^3J = 6 Hz, –CH_2 triazole); ^{13}C NMR (75 MHz, DMSO-d_6) δ (ppm): 183.5, 176.2 (C=S), 159.7, 158.2, 150.6, 142.9 (C=N azomethine), 141.9, 138.5, 137.0, 134.8, 129,7, 129.3, 128.9, 127.5, 126.3, 124.9, 124.7, 123.8, 118.0 (C≡N), 115.4, 115.1, 111.6, 66.6, 49.5, 35.4; LC-MS *m*/*z* 550 [M^-]; anal. calcd for $C_{28}H_{22}N_8O_3S$: C, 61.08; H, 4.03; N, 20.35; found: C, 60.97; H, 3.89; N, 20.18.

4.5.5 1-((4-(2-(4-((2,3-Dioxoindolin-1-yl)methyl)-1*H*-1,2,3-triazol-1-yl) ethoxy) phenyl)methylene)-4-phenylthiosemicarbazide (4e). Appearance: yellow solid; yield: 83%; melting point: 202–204 °C; R_f: 0.52 (*n*-hexane: EtOAc, 4 : 6); FT-IR $\bar{\nu}$ (cm^{-1}):3300 (N–H stretch), 3129, 3049 (C_{sp^2}–H stretch), 2928, 2873 (C_{sp^3}–H stretch), 1737 (C=O stretch, ketone), 1600 (C=O stretch, lactam), 1525 (C=N stretch, imine),1508 (C=C stretch, aromatic ring), 1467 (C_{sp^3}–H bend, methylene), 1274 (C_{sp^2}–O stretch, ether), 1201 (C–N stretch, lactam), 1165 (C_{sp^3}–O stretch, ether), 833 (C–H bend, 1,4-disubstitution), 755 (C–H bend, 1,2-disubstitution); ^{1}H NMR (300 MHz, DMSO-d_6) δ (ppm): 11.82 (s, 1*H*, –NH), 9.98 (s, 1*H*, –NH), 8.38 (s, 1*H*, –CH=N), 7.36 (s, 1*H*, –CH triazole), 8.37–6.89 (m, 13*H*, Ar–H), 5.13 (s, 2*H*, –CH_2 isatin), 4.71 (t, 2*H*, ^3J = 6 Hz, –OCH_2), 4.14 (t, 2*H*, ^3J = 6 Hz, –CH_2 triazole); ^{13}C NMR (75 MHz, DMSO-d_6) δ (ppm): 183.4, 161.8 (C=S), 160.2, 158.6, 150.6, 149.6, 142.9 (C=N azomethine), 139.7, 138.6, 129.6, 129.4, 127.3, 125.9, 124.9, 124.1, 123.7, 117.8, 115.5, 110.7, 61.6, 47.4, 35.4; LC-MS *m*/*z* 525 [M^-]; anal. calcd for $C_{27}H_{23}N_7O_3S$: C, 61.70; H, 4.41; N, 18.66; found: C, 61.56; H, 4.32; N, 18.43.

4.5.6 1-((4-(2-(4-((2,3-Dioxoindolin-1-yl)methyl)-1*H*-1,2,3-triazol-1-yl)ethoxy)- phenyl)methylene)-4-*p*-tolylthiosemicarbazide (4f). Appearance: yellow solid; yield: 85%; melting point: 207–209 °C; R_f: 0.46 (*n*-hexane: EtOAc, 4 : 6); FT-IR $\bar{\nu}$ (cm^{-1}):3300 (N–H stretch), 3129, 3049 (C_{sp^2}–H stretch), 2928, 2873 (C_{sp^3}–H stretch), 1731 (C=O stretch, ketone), 1612 (C=O stretch, lactam), 1541 (C=N stretch, imine), 1506 (C=C stretch, aromatic ring), 1469 (C_{sp^3}–H bend, methylene), 1271 (C_{sp^2}–O stretch, ether), 1214 (C–N stretch, lactam), 1170 (C_{sp^3}–O stretch, ether), 815 (C–H bend, 1,4-disubstitution), 756 (C–H bend, 1,2-disubstitution); ^{1}H NMR (300 MHz, DMSO-d_6) δ (ppm): 11.68 (s, 1*H*, –NH), 9.98 (s, 1*H*, –NH), 8.25 (s, 1*H*, –CH=N), 8.07 (s, 1*H*, –CH triazole), 7.81–6.89 (m, 12*H*, Ar–H), 4.97 (s, 2*H*, –CH_2 isatin), 4.74 (t, 2*H*, ^3J = 6 Hz, –OCH_2), 4.42 (t, 2*H*, ^3J = 6 Hz, –CH_2 triazole), 2.31 (s, 3*H*, –CH_3); ^{13}C NMR (75 MHz, DMSO-d_6) δ (ppm): 183.5, 176.2 (C=S), 159.7, 158.2, 150.6, 142.9 (C=N azomethine), 141.9, 138.5, 137.0, 134.8, 129.7, 129.3, 128.9, 127.5, 126.3, 124.9, 124.7, 123.8, 118.0, 115.4, 115.1, 111.6, 66.6, 49.5, 35.4, 21.0 (CH_3); LC-MS *m*/*z* 539 [M^-]; anal. calcd for $C_{28}H_{25}N_7O_3S$: C, 62.32; H, 4.67; N, 18.17; found: C, 62.13; H, 4.51; N, 18.01.

4.5.7 1-((4-(2-(4-((2,3-Dioxoindolin-1-yl)methyl)-1*H*-1,2,3-triazol-1-yl)ethoxy) phenyl)methylene)-4-(4-nitrophenyl) thiosemicarbazide (4g). Appearance: bright yellow solid; yield: 79%; melting point: 221–223 °C; R_f: 0.43 (*n*-hexane: EtOAc, 4 : 6); FT-IR $\bar{\nu}$ (cm^{-1}):3300 (N–H stretch), 3129, 3049 (C_{sp^2}–H stretch), 2928, 2873 (C_{sp^3}–H stretch), 1732 (C=O stretch, ketone), 1683 (C=O stretch, lactam), 1579 (C=N stretch, imine), 1556 (N–O stretch, asymmetric, nitro), 1508 (C=C stretch, aromatic ring), 1467 (C_{sp^3}–H bend, methylene), 1354 (N–O stretch, symmetric, nitro), 1244 (C_{sp^2}–O stretch, ether), 1219 (C–N stretch, lactam), 1165 (C_{sp^3}–O stretch, ether), 831 (C–H bend, 1,4-disubstitution), 758 (C–H bend, 1,2-disubstitution); ^{1}H NMR (300 MHz, DMSO-d_6) δ (ppm): 12.03 (s, 1*H*, –NH), 9.98 (s, 1*H*, –NH), 8.42–6.87 (m, 14*H*, CH=N, –CH triazole, Ar–H), 5.15 (s, 2*H*, –CH_2 isatin), 4.68 (t, 2*H*, ^3J = 6 Hz, –OCH_2), 4.14 (t, 2*H*, ^3J = 6 Hz, –CH_2 triazole); ^{13}C NMR (75 MHz, DMSO-d_6) δ (ppm): 183.4, 161.7 (C=S), 160.2, 158.6, 150.6, 149.6, 142.9 (C=N azomethine), 139.6, 138.6, 129.6, 129.4, 127.4, 125.9, 124.9, 124.1, 123.7, 117.8, 115.5, 110.6, 61.6, 47.4, 35.4; LC-MS *m*/*z* 570 [M^-]; anal. calcd for $C_{27}H_{22}N_8O_5S$: C, 56.84; H, 3.89; N, 19.64; found: C, 56.65; H, 3.71; N, 19.66.

4.5.8 1-((4-(2-(4-((2,3-Dioxoindolin-1-yl)methyl)-1*H*-1,2,3-triazol-1-yl)ethoxy) phenyl)methylene)-4-(4-cyanophenyl) thiosemicarbazide (4h). Appearance: yellow solid; yield: 87%; melting point: 226–228 °C; R_f: 0.41 (*n*-hexane: EtOAc, 4 : 6); FT-IR $\bar{\nu}$ (cm^{-1}):3300 (N–H stretch), 3129, 3049 (C_{sp^2}–H stretch), 2928, 2873 (C_{sp^3}–H stretch), 2250 (C≡N stretch, cyano) 1737 (C=O stretch, ketone), 1600 (C=O stretch, lactam), 1525 (C=N stretch, imine),1508 (C=C stretch, aromatic ring), 1467 (C_{sp^3}–H bend, methylene), 1274 (C_{sp^2}–O stretch, ether), 1201 (C–N stretch, lactam), 1165 (C_{sp^3}–O stretch, ether), 833 (C–H bend, 1,4-disubtitution), 755 (C–H bend, 1,2-disubstitution); ^{1}H NMR (300 MHz, DMSO-d_6) δ (ppm): 11.68 (s, 1*H*, –NH), 9.99 (s, 1*H*, –NH), 8.29–6.89 (m, 14*H*, –CH=N, –CH triazole Ar–H), 4.97 (s, 2*H*, –CH_2 isatin), 4.74 (t, 2*H*, ^3J = 6 Hz, –OCH_2), 4.42 (t, 2*H*, ^3J = 6 Hz, –CH_2 triazole); ^{13}C NMR (75 MHz, DMSO-d_6) δ (ppm): 183.5, 176.2 (C=S), 159.7, 158.2, 150.6, 142.9 (C=N azomethine), 141.9, 138.5, 137.0, 134.8, 129,7, 129.3, 128.9, 127.5, 126.3, 124.9, 124.7, 123.8, 118.0 (C≡N), 115.4, 115.1, 111.6,

66.6, 49.5, 35.4; LC-MS *m*/*z* 550 [M$^-$]; anal. calcd for $C_{28}H_{22}N_8O_3S$: C, 61.08; H, 4.03; N, 20.35; found: C, 60.86; H, 3.93; N, 20.54.

4.6 General procedure for the synthesis of isatin–triazole derived bis-thiosemicarbazones (5a–h)

To the stirred solution of isatin–triazole hybrids **3a** & **3b** (0.1 g, 0.27 mmol) respectively in ethanol, suitable N^4-substituted thiosemicarbazide **3c** (2.1 eq., 0.56 mmol) was added under vigorous stirring. The reaction was carried out for 6 hours heating under reflux and progress of reaction was monitored after regular intervals by TLC (*n*-hexane: EtOAc, 7 : 3). The precipitates formed upon completion, were filtered, washed, dried and recrystallized when required to give the pure product. By following this procedure, a series of bis-thiosemicarbazone derivatives **5a–h** of isatin–triazole hybrids **3a** & **3b** having different thiosemicarbazide moieties were synthesized.

4.6.1 1-((4-((1-(2-(Indolin-3(4-phenylthiosemicarbazon)-2-one-1-yl)ethyl)-1*H*-1,2,3-triazol-4-yl)methoxy)phenyl) methylene)-4-phenylthiosemicarbazide (5a). Appearance: orange yellow solid; yield: 79%; melting point: 202–204 °C; R_f: 0.52 (*n*-hexane: EtOAc, 4 : 6); FT-IR $\bar{\nu}$ (cm^{-1}):3300 (N–H stretch), 3129, 3049 (C_{sp^2}–H stretch), 2928, 2873 (C_{sp^3}–H stretch), 1600 (C=O stretch, lactam), 1544, 1525 (C=N stretch, imine),1487 (C=C stretch, aromatic ring), 1467 (C_{sp^3}–H bend, methylene), 1249 (C_{sp^2}–O stretch, ether), 1192 (C–N stretch, lactam), 1151 (C_{sp^3}–O stretch, ether), 827 (C–H bend, 1,4-disubstitution), 746 (C–H bend, 1,2-disubstitution); ^{1}H NMR (300 MHz, DMSO-d_6) δ (ppm): 12.56 (s, 1*H*, –NH), 11.73 (s, 1*H*, –NH), 10.88 (s, 1*H*, –NH), 10.05 (s, 1*H*, –NH), 8.29 (s, 1*H*, –CH=N), 8.11 (s, 1*H*, –CH triazole), 7.86–6.98 (m, 16*H*, Ar–H), 5.13 (s, 2*H*, –OCH_2), 4.73 (t, 2*H*, ^3J = 6 Hz, –CH_2-triazole), 4.25 (t, 2*H*, ^3J = 6 Hz, –CH_2-isatin); ^{13}C NMR ((75 MHz, DMSO-d_6) δ (ppm)): 183.3, 176.8 (C=S), 176.1 (C=S), 161.3, 160.1, 150.6, 143.2 (C=N imine), 142.9 (C=N azomethine), 139.5, 138.9, 131.7, 129.7, 128.9, 128.5, 127.3, 126.6, 126.3, 124.9, 123.7, 123.4, 121.6, 119.6, 117.8, 115.3, 110.7, 110.1, 61.5, 49.5, 35.1; LC-MS *m*/*z* 674 [M$^-$]; anal. calcd for $C_{34}H_{30}N_{10}O_2S_2$: C, 60.52; H, 4.48; N, 20.76; found: C, 60.41; H, 4.25; N, 20.81.

4.6.2 1-((4-((1-(2-(Indolin-3(*p*-tolylthiosemicarbazon)-2-one-1-yl)ethyl)-1*H*-1,2,3-triazol-4-yl)methoxy)phenyl)methylene)-*p*-totylthiosemicarbazide (5b). Appearance: yellow solid; yield: 82%; melting point: 207–209 °C; R_f: 0.54 (*n*-hexane: EtOAc, 4 : 6); FT-IR $\bar{\nu}$ (cm^{-1}):3300 (N–H stretch), 3129, 3049 (C_{sp^2}–H stretch), 2928, 2873 (C_{sp^3}–H stretch), 1610 (C=O stretch, lactam), 1540, 1516 (C=N stretch, imine), 1487 (C=C stretch, aromatic ring), 1467 (C_{sp^3}–H bend, methylene), 1249 (C_{sp^2}–O stretch, ether), 1197 (C–N stretch, lactam), 1151 (C_{sp^3}–O stretch, ether), 813 (C–H bend, 1,4-disubstitution), 746 (C–H bend, 1,2-disubstitution); ^{1}H NMR (300 MHz, DMSO-d_6) δ (ppm): 12.53 (s, 1*H*, –NH), 11.68 (s, 1*H*, –NH), 10.88 (s, 1*H*, –NH), 9.98 (s, 1*H*, –NH), 8.29 (s, 1*H*, –CH=N), 8.10 (s, 1*H*, –CH triazole), 7.86–6.98 (m, 16*H*, Ar–H), 5.13 (s, 2*H*, –OCH_2), 4.73 (t, 2*H*, ^3J = 6 Hz, –CH_2-triazole), 4.25 (t, 2*H*, ^3J = 6 Hz, –CH_2-isatin), 2.32 (s, 6*H*, –CH_3); ^{13}C NMR (75 MHz, DMSO-d_6) δ (ppm): 176.7 (C=S), 176.1 (C=S), 161.2, 160.0, 143.0 (C=N imine), 142.8 (C=N azomethine), 137.0, 136.3, 135.9, 134.8, 131.6, 131.2, 129.7, 129.3, 128.9, 127.3, 126.2, 126.1, 125.7, 123.4, 121.6, 119.6, 115.3, 110.1, 61.6, 47.4, 21.6, 21.1 (CH_3), 21.1 (CH_3); LC-MS *m*/*z* 702 [M$^-$]; anal. calcd for $C_{36}H_{34}N_{10}O_2S_2$: C, 61.52; H, 4.88; N, 19.93; found: C, 61.37; H, 4.96; N, 20.16.

4.6.3 1-((4-((1-(2-(Indolin-3(4-phenylthiosemicarbazon)-2-one-1-yl)ethyl)-1*H*-1,2,3-triazol-4-yl)methoxy)phenyl) methylene)-4-nitrophenylthiosemi-carbazide (5c). Appearance: bright yellow solid; yield: 76%; melting point: 232–234 °C; R_f: 0.60 (*n*-hexane: EtOAc, 4 : 6); FT-IR $\bar{\nu}$ (cm^{-1}):3300 (N–H stretch), 3129, 3049 (C_{sp^2}–H stretch), 2928, 2873 (C_{sp^3}–H stretch), 1600 (C=O stretch, lactam), 1544, 1525 (C=N stretch, imine), 1556 (N–O stretch, asymmetric, nitro), 1508 (C=C stretch, aromatic ring), 1467 (C_{sp^3}–H bend, methylene), 1354 (N–O stretch, symmetric, nitro), 1249 (C_{sp^2}–O stretch, ether), 1192 (C–N stretch, lactam), 1151 (C_{sp^3}–O stretch, ether), 827 (C–H bend, 1,4-disubstitution), 746 (C–H bend, 1,2-disubstitution); ^{1}H NMR (300 MHz, DMSO-d_6) δ (ppm): 12.71 (s, 1*H*, –NH), 11.73 (s, 1*H*, –NH), 10.90 (s, 1*H*, –NH), 10.05 (s, 1*H*, –NH), 8.27 (s, 1*H*, –CH=N), 8.25 (s, 1*H*, –CH triazole), 8.08–6.91 (m, 16*H*, Ar–H), 5.07 (s, 2*H*, –CH_2 isatin), 4.75 (t, 2*H*, ^3J = 6 Hz, –OCH_2), 4.43 (t, 2*H*, ^3J = 6 Hz, –CH_2 triazole); ^{13}C NMR (75 MHz, DMSO-d_6) δ (ppm): 176.5 (C=S), 175.4 (C=S), 172.5, 160.9, 160.0, 144.1, 143.9 (C=N imine), 143.2 (C=N azomethine), 141.9, 133.1, 132.7, 131.9, 129.9, 127.2, 125.6, 125.4, 124.9, 123.5, 121.8, 119.6, 119.5, 119.2, 115.2, 108.2, 107.1, 66.6, 49.5, 35.1; LC-MS *m*/*z* 764 [M$^-$]; anal. calcd for $C_{34}H_{28}N_{12}O_6S_2$: C, 53.40; H, 3.69; N, 21.98; found: C, 53.32; H, 3.57; N, 22.11.

4.6.4 1-((4-((1-(2-(Indolin-3(4-cyanophenylthiosemicarbazon)-2-one-1-yl)ethyl)-1*H*-1,2,3-triazol-4-yl) methoxy)phenyl)methylene)-4-(4-cyanophenyl) thiosemicarbazide (5d). Appearance: yellow solid; yield: 69%; melting point: 221–223 °C; R_f: 0.63 (*n*-hexane: EtOAc, 4 : 6); FT-IR $\bar{\nu}$ (cm^{-1}):3300 (N–H stretch), 3129, 3049 (C_{sp^2}–H stretch), 2928, 2873 (C_{sp^3}–H stretch), 2223 (C≡N stretch, cyano), 1604 (C=O stretch, lactam), 1585, 1537 (C=N stretch, imine), 1508 (C=C stretch, aromatic ring), 1465 (C_{sp^3}–H bend, methylene), 1249 (C_{sp^2}–O stretch, ether), 1192 (C–N stretch, lactam), 1151 (C_{sp^3}–O stretch, ether), 829 (C–H bend, 1,4-disubstitution), 750 (C–H bend, 1,2-disubstitution); ^{1}H NMR (300 MHz, DMSO-d_6) δ (ppm): 12.71 (s, 1*H*, –NH), 12.01 (s, 1*H*, –NH), 11.06 (s, 1*H*, –NH), 10.26 (s, 1*H*, –NH), 8.32 (s, 1*H*, –CH=N), 8.30 (s, 1*H*, –CH triazole), 8.14–6.99 (m, 16*H*, Ar–H), 5.14 (s, 2*H*, –OCH_2), 4.73 (t, 2*H*, ^3J = 6 Hz, –CH_2-triazole), 4.24 (t, 2*H*, ^3J = 6 Hz, –CH_2-isatin); ^{13}C NMR (75 MHz, DMSO-d_6) δ (ppm): 176.5 (C=S), 175.4 (C=S), 172.5, 160.9, 160.0, 144.1, 143.9 (C=N imine), 143.2 (C=N azomethine), 141.9, 133.1, 132.7, 131.9, 129.9, 127.2, 125.6, 125.4, 124.9, 123.5, 121.8, 119.6 (C≡N), 119.5 (C≡N), 119.2, 115.2, 108.2, 107.1, 66.7, 49.5, 35.1; LC-MS *m*/*z* 724 [M$^-$]; anal. calcd for $C_{36}H_{28}N_{12}O_2S_2$: C, 59.65; H, 3.89; N, 23.19; found: C, 59.49; H, 3.99; N, 23.32.

4.6.5 1-((4-(2-(4-((Indolin-3(4-phenylthiosemicarbazon)-2-one-1-yl)methyl)-1*H*-1,2,3-triazol-1-yl)ethoxy)phenyl) methylene)-4-phenylthiosemicarb-azide (5e). Appearance: bright yellow solid; yield: 81%; melting point: 232–234 °C; R_f: 0.51 (*n*-hexane: EtOAc, 4 : 6); FT-IR $\bar{\nu}$ (cm^{-1}):3300 (N–H stretch), 3129, 3049 (C_{sp^2}–H stretch), 2928, 2873 (C_{sp^3}–H stretch), 1608

(C=O stretch, lactam), 1544, 1525 (C=N stretch, imine),1492 (C=C stretch, aromatic ring), 1465 (C_{sp^3}–H bend, methylene), 1244 (C_{sp^2}–O stretch, ether), 1192 (C–N stretch, lactam), 1141 (C_{sp^3}–O stretch, ether), 827 (C–H bend, 1,4-disubstitution), 740 (C–H bend, 1,2-disubstitution); ^{1}H NMR (300 MHz, DMSO-d_6) δ (ppm): 12.71 (s, 1*H*, –NH), 11.73 (s, 1*H*, –NH), 10.89 (s, 1*H*, –NH), 10.05 (s, 1*H*, –NH), 8.27 (s, 1*H*, –CH=N), 8.09 (s, 1*H*, –CH triazole), 7.83–6.91 (m, 18*H*, Ar–H), 5.07 (s, 2*H*, –CH_2 isatin), 4.75 (t, 2*H*, ^3J = 6 Hz, –OCH_2), 4.43 (t, 2*H*, ^3J = 6 Hz, –CH_2 triazole); ^{13}C NMR (75 MHz, DMSO-d_6) δ (ppm): 176.8 (C=S), 176.1 (C=S), 160.9, 159.8, 143.1 (C=N imine), 142.9 (C=N azomethine), 141.9, 139.5, 138.8, 131.6, 131.5, 129.7, 128.9, 128.4, 127.5, 126.6, 126.3, 126.1, 125.7, 124.8, 123.5, 121.6, 119.8, 115.2, 110.9, 66.6, 49.5, 35.1; LC-MS *m*/*z* 674 [M$^-$]; anal. calcd for $C_{34}H_{30}N_{10}O_2S_2$: C, 60.52; H, 4.48; N, 20.76; found: C, 60.61; H, 4.29; N, 20.87.

4.6.6 1-((4-(2-(4-((Indolin-3(*p*-tolylthiosemicarbazon)-2-one-1-yl)methyl)-1*H*-1,2,3-triazol-1-yl)ethoxy)phenyl)methylene)-*p*-tolylthiosemicarbazide (5f). Appearance: yellow solid; yield: 83%; melting point: 236–238 °C; R_f: 0.54 (*n*-hexane: EtOAc, 4 : 6); FT-IR $\bar{\nu}$ (cm^{-1}):3300 (N–H stretch), 3129, 3049 (C_{sp^2}–H stretch), 2928, 2873 (C_{sp^3}–H stretch), 1612 (C=O stretch, lactam), 1544, 1539 (C=N stretch, imine), 1487 (C=C stretch, aromatic ring), 1467 (C_{sp^3}–H bend, methylene), 1271 (C_{sp^2}–O stretch, ether), 1193 (C–N stretch, lactam), 1151 (C_{sp^3}–O stretch, ether), 813 (C–H bend, 1,4-disubstitution), 750 (C–H bend, 1,2-disubstitution); ^{1}H NMR (300 MHz, DMSO-d_6) δ (ppm): 12.68 (s, 1*H*, –NH), 11.68 (s, 1*H*, –NH), 10.83 (s, 1*H*, –NH), 9.98 (s, 1*H*, –NH), 8.27 (s, 1*H*, –CH=N), 8.25 (s, 1*H*, –CH triazole), 8.07–6.89 (m, 16*H*, Ar–H), 5.07 (s, 2*H*, ^3J = 6 Hz, –CH_2 isatin), 4.75 (t, 2*H*, ^3J = 6 Hz, –OCH_2), 4.43 (t, 2*H*, –CH_2 triazole), 2.32 (s, 6*H*, –CH_3); ^{13}C NMR (75 MHz, DMSO-d_6) δ (ppm): 176.2 (C=S), 176.1 (C=S), 160.9, 159.8, 158.2, 150.6, 142.9 (C=N imine), 141.9 (C=N azomethine), 138.5, 137.0, 136.3, 135.9, 134.8, 131.6, 129.7, 129.3, 128.9, 127.5, 126.3, 126.1, 124.9, 124.7, 123.8, 123.5, 118.0, 115.2, 111.6, 66.7, 49.5, 35.1, 21.6 (CH_3), 21.0 (CH_3); LC-MS *m*/*z* 702 [M$^-$]; anal. calcd for $C_{36}H_{34}N_{10}O_2S_2$: C, 61.52; H, 4.88; N, 19.93; found: C, 61.35; H, 4.74; N, 19.89.

4.6.7 1-((4-(2-(4-((Indolin-3(4-nitrophenylthiosemicarbazon)-2-one-1-yl) methyl)-1*H*-1,2,3-triazol-1-yl)ethoxy)phenyl)methylene)-4-nitrophenyl thiosemicarbazide (5g). Appearance: yellow; yield: 75%; melting point: 252–254 °C; R_f: 0.59 (*n*-hexane: EtOAc, 4 : 6); FT-IR $\bar{\nu}$ (cm^{-1}):3300 (N–H stretch), 3129, 3049 (C_{sp^2}–H stretch), 2928, 2873 (C_{sp^3}–H stretch), 1612 (C=O stretch, lactam), 1544, 1539 (C=N stretch, imine), 1556 (N–O stretch, asymmetric, nitro), 1508 (C=C stretch, aromatic ring), 1467 (C_{sp^3}–H bend, methylene), 1354 (N–O stretch, symmetric, nitro), 1271 (C_{sp^2}–O stretch, ether), 1193 (C–N stretch, lactam), 1151 (C_{sp^3}–O stretch, ether), 813 (C–H bend, 1,4-disubstitution), 750 (C–H bend, 1,2-disubstitution); ^{1}H NMR (300 MHz, DMSO-d_6) δ (ppm): 12.90 (s, 1*H*, –NH), 12.09 (s, 1*H*, –NH), 11.18 (s, 1*H*, –NH), 10.37 (s, 1*H*, –NH), 8.31–6.89 (m, 18*H*, –CH=N, –CH triazole, Ar–H), 5.07 (s, 2*H*, –CH_2 isatin), 4.97 (t, 2*H*, ^3J = 6 Hz, –OCH_2), 4.76 (t, 2*H*, ^3J = 6 Hz, –CH_2 triazole); ^{13}C NMR (75 MHz, DMSO-d_6) δ (ppm): 176.5 (C=S), 175.4 (C=S), 172.5, 160.9, 160.0, 144.1, 143.9 (C=N imine), 143.2 (C=N azomethine), 141.9, 133.1, 132.7, 131.9, 129.9, 127.2, 125.6, 125.4, 124.9, 123.5, 121.8, 119.6, 119.5, 119.2, 115.2, 108.2, 107.1, 66.7, 49.5, 35.1; LC-MS *m*/*z* 764 [M$^-$]; anal. calcd for $C_{34}H_{28}N_{12}O_6S_2$: C, 53.40; H, 3.69; N, 21.98; found: C, 53.53; H, 3.78; N, 21.69.

4.6.8 1-((4-(2-(4-((Indolin-3(4-cyanophenylthiosemicarbazon)-2-one-1-yl) methyl)-1*H*-1,2,3-triazol-1-yl)ethoxy)phenyl)methylene)-4-cyanophenyl thiosemicarbazide (5h). Appearance: bright yellow solid; yield: 79%; melting point: 258–260 °C; R_f: 0.62 (*n*-hexane: EtOAc, 4 : 6); FT-IR $\bar{\nu}$ (cm^{-1}):3300 (N–H stretch), 3129, 3049 (C_{sp^2}–H stretch), 2928, 2873 (C_{sp^3}–H stretch), 2223 (C≡N stretch, cyano), 1604 (C=O stretch, lactam), 1585, 1537 (C=N stretch, imine),1508 (C=C stretch, aromatic ring), 1465 (C_{sp^3}–H bend, methylene), 1249 (C_{sp^2}–O stretch, ether), 1192 (C–N stretch, lactam), 1151 (C_{sp^3}–O stretch, ether), 829 (C–H bend, 1,4-disubstitution), 750 (C–H bend, 1,2-disubstitution); ^{1}H NMR (300 MHz, DMSO-d_6) δ (ppm): 12.86 (s, 1*H*, –NH), 12.01 (s, 1*H*, –NH), 11.08 (s, 1*H*, –NH), 10.26 (s, 1*H*, –NH), 8.27 (s, 1*H*, –CH=N), 8.25 (s, 1*H*, –CH triazole), 8.12–6.93 (m, 16*H*, Ar–H), 5.07 (s, 2*H*, –CH_2 isatin), 4.77 (t, 2*H*, ^3J = 6 Hz, –OCH_2), 4.44 (t, 2*H*, ^3J = 6 Hz, –CH_2 triazole); ^{13}C NMR (75 MHz, DMSO-d_6) δ (ppm): 176.5 (C=S), 175.4 (C=S), 172.5, 160.9, 160.0, 144.1, 143.9 (C=N imine), 143.2 (C=N azomethine), 141.9, 133.1, 132.7, 131.9, 129.9, 127.2, 125.6, 125.4, 124.9, 123.5, 121.8, 119.6 (C≡N), 119.5 (C≡N), 119.2, 115.2, 108.2, 107.0, 66.6, 49.5, 35.1; LC-MS *m*/*z* 724 [M$^-$]; anal. calcd for $C_{36}H_{28}N_{12}O_2S_2$: C, 59.65; H, 3.89; N, 23.19; found: C, 59.48; H, 3.75; N, 23.33.

Conflicts of interest

There are no conflicts to declare.

Acknowledgements

We are highly grateful to the Department of Chemistry, Quaid-i-Azam University for financial support under URF; we also thank "The World Academy of Sciences (TWAS)" for financial support (Project No. 13–419 RG/PHA/AS_CUNESCO FR: 3240279216).

References

1 A. Mushtaq, P. Wu and M. M. Naseer, Recent drug design strategies and identification of key heterocyclic scaffolds for promising anticancer targets, *Pharmacol. Ther.*, 2024, **254**, 108579.

2 B. Eftekhari-Sis, M. Zirak and A. Akbari, Arylglyoxals in synthesis of heterocyclic compounds, *Chem. Rev.*, 2013, **113**(5), 2958–3043.

3 T. Al-Warhi, D. M. Elimam, Z. M. Elsayed, M. M. Abdel-Aziz, R. M. Maklad, A. A. Al-Karmalawy, K. Afarinkia, M. A. Abourehab, H. A. Abdel-Aziz and W. M. Eldehna, Development of novel isatin thiazolyl-pyrazoline hybrids as promising antimicrobials in MDR pathogens, *RSC Adv.*, 2022, **12**(48), 31466–31477.

4 Y. Wang, Z. Liang, Y. Zheng, A. S.-L. Leung, S.-C. Yan, P.-K. So, Y.-C. Leung, W.-L. Wong and K.-Y. Wong, Rational structural modification of the isatin scaffold to

develop new and potent antimicrobial agents targeting bacterial peptidoglycan glycosyltransferase, *RSC Adv.*, 2021, **11**(29), 18122–18130.

5 A. Katiyar, M. Hegde, S. Kumar, V. Gopalakrishnan, K. D. Bhatelia, K. Ananthaswamy, S. A. Ramareddy, E. De Clercq, B. Choudhary and D. Schols, Synthesis and evaluation of the biological activity of N′-[2-oxo-1, 2 dihydro-3 H-indol-3-ylidene] benzohydrazides as potential anticancer agents, *RSC Adv.*, 2015, **5**(56), 45492–45501.

6 L. Zhang, F. Chen, J. Wang, Y. Chen, Z. Zhang, Y. Lin and X. Zhu, Novel isatin derivatives of podophyllotoxin: synthesis and cytotoxic evaluation against human leukaemia cancer cells as potent anti-MDR agents, *RSC Adv.*, 2015, **5**(118), 97816–97823.

7 A. M. Hamdy, N. A. Al-Masoudi, C. Pannecouque, Q. Rahman, A. Villinger and P. Langer, Regioselective Suzuki–Miyaura reactions of 4, 7-dichloro-N-methylisatin. Synthesis, anti-HIV activity and modeling study, *RSC Adv.*, 2015, **5**(130), 107360–107369.

8 L. Emami, L. Moezi, L. Amiri-Zirtol, F. Pirsalami, M. Divar, A. Solhjoo and S. Khabnadideh, Anticonvulsant activity, molecular modeling and synthesis of spirooxindole-4 H-pyran derivatives using a novel reusable organocatalyst, *Mol. Diversity*, 2022, **26**(6), 3129–3141.

9 R. Nath, S. Pathania, G. Grover and M. J. Akhtar, Isatin containing heterocycles for different biological activities: Analysis of structure activity relationship, *J. Mol. Struct.*, 2020, **1222**, 128900.

10 J. Haribabu, G. Subhashree, S. Saranya, K. Gomathi, R. Karvembu and D. Gayathri, Isatin based thiosemicarbazone derivatives as potential bioactive agents: Anti-oxidant and molecular docking studies, *J. Mol. Struct.*, 2016, **1110**, 185–195.

11 A. S. Hassan, N. M. Morsy, W. M. Aboulthana and A. Ragab, Exploring novel derivatives of isatin-based Schiff bases as multi-target agents: design, synthesis, in vitro biological evaluation, and in silico ADMET analysis with molecular modeling simulations, *RSC Adv.*, 2023, **13**(14), 9281–9303.

12 Q. U. Ain, A. Singh, I. Singh, R. Carmieli and R. Sharma, Synthesis, characterization and anti-tubercular activities of copper (II) complexes of substituted 2, 3-isatin bisthiosemicarbazones: An experimental and theoretical approach, *Results Chem.*, 2023, **6**, 101171.

13 S. K. Kancharla, S. Birudaraju, A. Pal, L. K. Reddy, E. R. Reddy, S. K. Vagolu, D. Sriram, K. B. Bonige and R. B. Korupolu, Synthesis and biological evaluation of isatin oxime ether-tethered aryl 1 H-1, 2, 3-triazoles as inhibitors of Mycobacterium tuberculosis, *New J. Chem.*, 2022, **46**(6), 2863–2874.

14 M. Ahmad, H. Pervez, S. Zaib, M. Yaqub, M. M. Naseer, S. U. Khan and J. Iqbal, Synthesis, biological evaluation and docking studies of some novel isatin-3-hydrazonothiazolines, *RSC Adv.*, 2016, **6**(65), 60826–60844.

15 S. Mehreen, M. Zia, A. Khan, J. Hussain, S. Ullah, M. U. Anwar, A. Al-Harrasi and M. M. Naseer, Phenoxy pendant isatins as potent α-glucosidase inhibitors: reciprocal carbonyl⋯ carbonyl interactions, antiparallel π⋯ π stacking driven solid state self-assembly and biological evaluation, *RSC Adv.*, 2022, **12**(32), 20919–20928.

16 A. Mushtaq, U. Azam, S. Mehreen and M. M. Naseer, Synthetic α-glucosidase inhibitors as promising anti-diabetic agents: Recent developments and future challenges, *Eur. J. Med. Chem.*, 2023, **249**, 115119.

17 S. Deswal, R. K. Tittal, D. G. Vikas, K. Lal and A. Kumar, 5-Fluoro-1H-indole-2, 3-dione-triazoles-synthesis, biological activity, molecular docking, and DFT study, *J. Mol. Struct.*, 2020, **1209**, 127982.

18 B. Posocco, M. Buzzo, L. Giodini, S. Crotti, S. D'Aronco, P. Traldi, M. Agostini, E. Marangon and G. Toffoli, Analytical aspects of sunitinib and its geometric isomerism towards therapeutic drug monitoring in clinical routine, *J. Pharm. Biomed. Anal.*, 2018, **160**, 360–367.

19 M. D. Hall, K. R. Brimacombe, M. S. Varonka, K. M. Pluchino, J. K. Monda, J. Li, M. J. Walsh, M. B. Boxer, T. H. Warren, H. M. Fales and M. M. Gottesman, Synthesis and Structure–Activity Evaluation of Isatin-β-thiosemicarbazones with Improved Selective Activity toward Multidrug-Resistant Cells Expressing P-Glycoprotein, *J. Med. Chem.*, 2011, **54**(16), 5878–5889.

20 B. Aneja, N. S. Khan, P. Khan, A. Queen, A. Hussain, M. T. Rehman, M. F. Alajmi, H. R. El-Seedi, S. Ali, M. I. Hassan and M. Abid, Design and development of Isatin-triazole hydrazones as potential inhibitors of microtubule affinity-regulating kinase 4 for the therapeutic management of cell proliferation and metastasis, *Eur. J. Med. Chem.*, 2019, **163**, 840–852.

21 S. N. A. Bukhari, T. G. Alsahli, H. Ejaz, N. Ahmed, W. Ahmad, M. A. Elsherif, N. H. Alotaibi, K. Junaid and N. Janković, Dual activity of indolin-2-ones containing an arylidene motif: DNA and BSA interaction, *RSC Adv.*, 2023, **13**(40), 28139–28147.

22 K. K. Saini, R. K. Upadhyay, R. Kant, A. Vajpayee, K. Jain, A. Kumar, L. S. Kumar and R. Kumar, Design, synthesis, molecular docking and DFT studies on novel melatonin and isatin based azole derivatives, *RSC Adv.*, 2023, **13**(39), 27525–27534.

23 H. A. Radwan, I. Ahmad, I. M. Othman, M. A. Gad-Elkareem, H. Patel, K. Aouadi, M. Snoussi and A. Kadri, Design, synthesis, in vitro anticancer and antimicrobial evaluation, SAR analysis, molecular docking and dynamic simulation of new pyrazoles, triazoles and pyridazines based isoxazole, *J. Mol. Struct.*, 2022, **1264**, 133312.

24 P. Chopade and A. Shaikh, Advancements and Future Perspectives of 1, 2, 3 Triazole Scaffold as Promising Antiviral Agent in Drug Discovery, *Int. J. Pharm. Sci. Res.*, 2022, 4805–4818.

25 N. Jangir, S. K. Bagaria and D. K. Jangid, Nanocatalysts: applications for the synthesis of N-containing five-membered heterocycles, *RSC Adv.*, 2022, **12**(30), 19640–19666.

26 R. Dharavath, N. Nagaraju, M. R. Reddy, D. Ashok, M. Sarasija, M. Vijjulatha, T. Vani, K. Jyothi and G. Prashanthi, Microwave-assisted synthesis, biological

evaluation and molecular docking studies of new coumarin-based 1, 2, 3-triazoles, *RSC Adv.*, 2020, **10**(20), 11615–11623.

27 A. Nandikolla, S. Srinivasarao, B. K. Kumar, S. Murugesan, H. Aggarwal, L. L. Major, T. K. Smith and K. V. G. C. Sekhar, Synthesis, study of antileishmanial and antitrypanosomal activity of imidazo pyridine fused triazole analogues, *RSC Adv.*, 2020, **10**(63), 38328–38343.

28 A. Rani, G. Singh, A. Singh, U. Maqbool, G. Kaur and J. Singh, CuAAC-ensembled 1, 2, 3-triazole-linked isosteres as pharmacophores in drug discovery, *RSC Adv.*, 2020, **10**(10), 5610–5635.

29 H. A. Abuelizz, H. M. Awad, M. Marzouk, F. A. Nasr, A. S. Alqahtani, A. H. Bakheit, A. M. Naglah and R. Al-Salahi, Synthesis and biological evaluation of 4-(1 H-1, 2, 4-triazol-1-yl) benzoic acid hybrids as anticancer agents, *RSC Adv.*, 2019, **9**(33), 19065–19074.

30 K. Bhagat, J. V. Singh, A. Sharma, A. Kaur, N. Kumar, H. K. Gulati, A. Singh, H. Singh and P. M. S. Bedi, Novel series of triazole containing coumarin and isatin based hybrid molecules as acetylcholinesterase inhibitors, *J. Mol. Struct.*, 2021, **1245**, 131085.

31 A. Kumar, Y. Rohila, V. Kumar and K. Lal, A Mini Review on Pharmacological Significance of Isatin-1, 2, 3-Triazole Hybrids, *Curr. Top. Med. Chem.*, 2023, **23**(10), 833–847.

32 B. Aneja, N. S. Khan, P. Khan, A. Queen, A. Hussain, M. T. Rehman, M. F. Alajmi, H. R. El-Seedi, S. Ali and M. I. Hassan, Design and development of Isatin-triazole hydrazones as potential inhibitors of microtubule affinity-regulating kinase 4 for the therapeutic management of cell proliferation and metastasis, *Eur. J. Med. Chem.*, 2019, **163**, 840–852.

33 N. Busto, J. Leitão-Castro, A. T. García-Sosa, F. Cadete, C. S. Marques, R. Freitas and A. J. Burke, N-1, 2, 3-Triazole–isatin derivatives: anti-proliferation effects and target identification in solid tumour cell lines, *RSC Med. Chem.*, 2022, **13**(8), 970–977.

34 N. Rezki, M. A. Almehmadi, S. Ihmaid, A. M. Shehata, A. M. Omar, H. E. Ahmed and M. R. Aouad, Novel scaffold hopping of potent benzothiazole and isatin analogues linked to 1, 2, 3-triazole fragment that mimic quinazoline epidermal growth factor receptor inhibitors: Synthesis, antitumor and mechanistic analyses, *Bioorg. Chem.*, 2020, **103**, 104133.

35 R. Kumar and P. Takkar, Repositioning of Isatin hybrids as novel anti-tubercular agents overcoming pre-existing antibiotics resistance, *Med. Chem. Res.*, 2021, **30**, 847–876.

36 A. Kumar, K. Lal, M. Yadav, S. Kumar, M. B. Singh and K. Kumari, Isatin-semicarbazone linked acetamide 1, 2, 3-triazole hybrids: Synthesis, antimicrobial evaluation and docking simulations, *J. Mol. Struct.*, 2023, **1287**, 135660.

37 B. Shakya and P. N. Yadav, Thiosemicarbazones as potent anticancer agents and their modes of action, *Mini-Rev. Med. Chem.*, 2020, **20**(8), 638–661.

38 N. Balakrishnan, J. Haribabu, M. Dharmasivam, J. P. Jayadharini, D. Anandakrishnan, S. Swaminathan, N. Bhuvanesh, C. Echeverria and R. Karvembu, Influence of Indole-N substitution of thiosemicarbazones in cationic Ru (II)(η6-Benzene) complexes on their anticancer activity, *Organometallics*, 2023, **42**(3), 259–275.

39 D. L. Sun, S. Poddar, R. D. Pan, E. W. Rosser, E. R. Abt, J. Van Valkenburgh, T. M. Le, V. Lok, S. P. Hernandez and J. Song, Isoquinoline thiosemicarbazone displays potent anticancer activity with in vivo efficacy against aggressive leukemias, *RSC Med. Chem.*, 2020, **11**(3), 392–410.

40 B. Z. Sibuh, P. K. Gupta, P. Taneja, S. Khanna, P. Sarkar, S. Pachisia, A. A. Khan, N. K. Jha, K. Dua and S. K. Singh, Synthesis, in silico study, and anti-cancer activity of thiosemicarbazone derivatives, *Biomedicines*, 2021, **9**(10), 1375.

41 F. Pape Veronika, A. Enyedy Éva, K. Keppler Bernhard and R. Kowol Christian, Anticancer thiosemicarbazones: chemical properties, interaction with iron metabolism, and resistance development, *Antioxid. Redox Signaling*, 2019, **30**, 1062–1082.

42 N. K. Singh, A. A. Kumbhar, Y. R. Pokharel and P. N. Yadav, Anticancer potency of copper (II) complexes of thiosemicarbazones, *J. Inorg. Biochem.*, 2020, **210**, 111134.

43 B. Sever, G. Akalın Çiftçi, A. Özdemir and M. Altıntop, Design, synthesis and in vitro evaluation of new thiosemicarbazone derivatives as potential anticancer agents, *J. Res. Pharm.*, 2019, **23**(1), 16–24.

44 A. Mirzaahmadi, S. A. Hosseini-Yazdi, E. Safarzadeh, B. Baradaran, E. Samolova and M. Dusek, New series of water-soluble thiosemicarbazones and their copper (II) complexes as potentially promising anticancer compounds, *J. Mol. Liq.*, 2019, **293**, 111412.

45 S. J. Sardroud, S. A. Hosseini-Yazdi, M. Mahdavi, M. Poupon and E. Skorepova, Synthesis, characterization and in vitro evaluation of anticancer activity of a new water-soluble thiosemicarbazone ligand and its complexes, *Polyhedron*, 2020, **175**, 114218.

46 V. Manakkadan, J. Haribabu, V. N. V. Palakkeezhillam, P. Rasin, M. Mandal, V. S. Kumar, N. Bhuvanesh, R. Udayabhaskar and A. Sreekanth, Synthesis and characterization of N4-substituted thiosemicarbazones: DNA/BSA binding, molecular docking, anticancer activity, ADME study and computational investigations, *J. Mol. Struct.*, 2023, **1285**, 135494.

47 J. Haribabu, N. Balakrishnan, S. Swaminathan, D. P. Dorairaj, M. Azam, M. K. M. Subarkhan, Y.-L. Chang, S. C. Hsu, P. Štarha and R. Karvembu, Michael addition-driven synthesis of cytotoxic palladium (ii) complexes from chromone thiosemicarbazones: investigation of anticancer activity through in vitro and in vivo studies, *New J. Chem.*, 2023, **47**(33), 15748–15759.

48 K. Preetha, E. Seena, P. K. Maniyampara, E. Manoj and M. P. Kurup, Synthesis, crystal structure, Hirshfeld surface analysis, DFT, molecular docking and in vitro antitumor studies of (2E)-2-[4-(diethylamino) benzylidene]-N-ethylhydrazinecarbothioamide, *J. Mol. Struct.*, 2024, **1295**, 136700.

49 Y. Zou, Q. Zhao, J. Liao, H. Hu, S. Yu, X. Chai, M. Xu and Q. Wu, New triazole derivatives as antifungal agents:

Synthesis via click reaction, in vitro evaluation and molecular docking studies, *Bioorg. Med. Chem. Lett.*, 2012, **22**(8), 2959–2962.

50 K. Vine, L. Matesic, J. Locke, M. Ranson and D. Skropeta, Cytotoxic and anticancer activities of isatin and its derivatives: a comprehensive review from 2000-2008, *Anti-Cancer Agents Med. Chem.*, 2009, **9**(4), 397–414.

51 A. K. Gupta, S. Tulsyan, M. Bharadwaj and R. Mehrotra, Systematic review on cytotoxic and anticancer potential of n-substituted isatins as novel class of compounds useful in multidrug-resistant cancer therapy: In silico and in vitro analysis, *Top. Curr. Chem.*, 2019, **377**, 1–21.

52 M. Serafini, T. Pirali and G. C. Tron, Click 1, 2, 3-triazoles in drug discovery and development: From the flask to the clinic?, *Adv. Heterocycl. Chem.*, 2021, **134**, 101–148.

53 E. M. Othman, E. A. Fayed, E. M. Husseiny and H. S. Abulkhair, Rationale design, synthesis, cytotoxicity evaluation, and in silico mechanistic studies of novel 1, 2, 3-triazoles with potential anticancer activity, *New J. Chem.*, 2022, **46**(25), 12206–12216.

54 Y. Yu, D. S. Kalinowski, Z. Kovacevic, A. R. Siafakas, P. J. Jansson, C. Stefani, D. B. Lovejoy, P. C. Sharpe, P. V. Bernhardt and D. R. Richardson, Thiosemicarbazones from the old to new: iron chelators that are more than just ribonucleotide reductase inhibitors, *J. Med. Chem.*, 2009, **52**(17), 5271–5294.

55 P. Singh, P. Sharma, A. Anand, P. Bedi, T. Kaur, A. Saxena and V. Kumar, Azide-alkyne cycloaddition en route to novel 1H-1, 2, 3-triazole tethered isatin conjugates with in vitro cytotoxic evaluation, *Eur. J. Med. Chem.*, 2012, **55**, 455–461.

56 A. Shukla, Synthesis and biological screening of benzimidazole derivatives, *Int. J. Pharm. Sci. Res.*, 2012, **3**(3), 922.

57 S. J. Pitman, A. K. Evans, R. T. Ireland, F. Lempriere and L. K. McKemmish, Benchmarking basis sets for density functional theory thermochemistry calculations: Why unpolarized basis sets and the polarized 6-311G family should be avoided, *J. Phys. Chem. A*, 2023, **127**(48), 10295–10306.

58 N. Johnee Britto, M. Panneerselvam, M. Deepan Kumar, A. Kathiravan and M. Jaccob, Substituent Effect on the Photophysics and ESIPT Mechanism of N, N′-Bis (salicylidene)-p-phenylenediamine: A DFT/TD-DFT Analysis, *J. Chem. Inf. Model.*, 2021, **61**(4), 1825–1839.

59 P. Bianchi and J.-C. M. Monbaliu, Three decades of unveiling the complex chemistry of C-nitroso species with computational chemistry, *Org. Chem. Front.*, 2022, **9**(1), 223–264.

60 S. H. Sumrra, F. Mushtaq, F. Ahmad, R. Hussain, W. Zafar, M. Imran and M. N. Zafar, Coordination behavior, structural, statistical and theoretical investigation of biologically active metal-based isatin compounds, *Chem. Pap.*, 2022, **76**(6), 3705–3727.

61 K. Kaavin, D. Naresh, M. Yogeshkumar, M. K. Prakash, S. Janarthanan, M. M. Krishnan and M. Malathi, In-silico DFT studies and molecular docking evaluation of benzimidazo methoxy quinoline-2-one ligand and its Co, Ni, Cu and Zn complexes as potential inhibitors of Bcl-2, Caspase-3, EGFR, mTOR, and PI3K, cancer-causing proteins, *Chem. Phys. Impact.*, 2024, **8**, 100418.

62 M. Miar, A. Shiroudi, K. Pourshamsian, A. R. Oliaey and F. Hatamjafari, Theoretical investigations on the HOMO–LUMO gap and global reactivity descriptor studies, natural bond orbital, and nucleus-independent chemical shifts analyses of 3-phenylbenzo [d] thiazole-2 (3 H)-imine and its para-substituted derivatives: Solvent and substituent effects, *J. Chem. Res.*, 2021, **45**(1–2), 147–158.

63 Y. Wu and W. Zhu, Organic sensitizers from D–π–A to D–A–π–A: effect of the internal electron-withdrawing units on molecular absorption, energy levels and photovoltaic performances, *Chem. Soc. Rev.*, 2013, **42**(5), 2039–2058.

64 P. Udhayakalaa, T. V. Rajendiranb and S. Gunasekaran, Density functional theory investigations for the adsorption of some oxadiazole derivatives on mild steel, *J. Adv. Sci. Res.*, 2012, **3**(03), 67–74.

65 A. H. Radhi, E. A. Du, F. A. Khazaal, Z. M. Abbas, O. H. Aljelawi, S. D. Hamadan, H. A. Almashhadani and M. M. Kadhim, HOMO-LUMO energies and geometrical structures effecton corrosion inhibition for organic compounds predict by DFT and PM3 methods, *NeuroQuantology*, 2020, **18**(1), 37.

66 M. Akram, M. Adeel, M. Khalid, M. N. Tahir, M. U. Khan, M. A. Asghar, M. A. Ullah and M. Iqbal, A combined experimental and computational study of 3-bromo-5-(2, 5-difluorophenyl) pyridine and 3, 5-bis (naphthalen-1-yl) pyridine: Insight into the synthesis, spectroscopic, single crystal XRD, electronic, nonlinear optical and biological properties, *J. Mol. Struct.*, 2018, **1160**, 129–141.

67 A. Miličević, G. Miletić and I. N. Jovanović, Electrochemical oxidation of flavonoids: PM6 and DFT for elucidating electronic changes and modelling oxidation potential (part II), *J. Mol. Liq.*, 2019, **295**, 111730.

68 V. Choudhary, A. Bhatt, D. Dash and N. Sharma, DFT calculations on molecular structures, HOMO–LUMO study, reactivity descriptors and spectral analyses of newly synthesized diorganotin (IV) 2-chloridophenylacetohydroxamate complexes, *J. Comput. Chem.*, 2019, **40**(27), 2354–2363.

69 T. Kar, S. Scheiner and A. Sannigrahi, Hardness and Chemical Potential Profiles for Some Open-Shell HAB→HBA Type Reactions. Ab Initio and Density Functional Study, *J. Phys. Chem. A*, 1998, **102**(29), 5967–5973.

70 L. F. Dechouk, A. Bouchoucha, Y. Abdi, K. S. Larbi, A. Bouzaheur and S. Terrachet-Bouaziz, Coordination of new palladium (II) complexes with derived furopyran-3, 4-dione ligands: Synthesis, characterization, redox behaviour, DFT, antimicrobial activity, molecular docking and ADMET studies, *J. Mol. Struct.*, 2022, **1257**, 132611.

71 N.-B. Sun, J.-Q. Fu, J.-Q. Weng, J.-Z. Jin, C.-X. Tan and X.-H. Liu, Microwave assisted synthesis, antifungal activity and DFT theoretical study of some novel 1, 2, 4-triazole derivatives containing the 1, 2, 3-thiadiazole moiety, *Molecules*, 2013, **18**(10), 12725–12739.

72 M. Asiri, Synthesis, crystal structure and spectroscopic properties of 1, 2-benzothiazine derivatives: An experimental and DFT study, *Struct. Chem.*, 2015, **34**(1), 15–25.

73 M. N. Arshad, A. M. Asiri, K. A. Alamry, T. Mahmood, M. A. Gilani, K. Ayub and A. S. Birinji, Synthesis, crystal structure, spectroscopic and density functional theory (DFT) study of N-[3-anthracen-9-yl-1-(4-bromo-phenyl)-allylidene]-N-benzenesulfonohydrazine, *Spectrochim. Acta, Part A*, 2015, **142**, 364–374.

74 R. Galeazzi, C. Marucchini, M. Orena and C. Zadra, Stereoelectronic properties and activity of some imidazolinone herbicides: a computational approach, *J. Mol. Struct.*, 2003, **640**(1–3), 191–200.

75 A. Mahal, M. Al-Janabi, V. Eyüpoğlu, A. Alkhouri, S. Chtita, M. M. Kadhim, A. J. Obaidullah, J. M. Alotaibi, X. Wei and M. R. F. Pratama, Molecular docking, drug-likeness and DFT study of some modified tetrahydrocurcumins as potential anticancer agents, *Saudi Pharm. J.*, 2024, **32**(1), 101889.

76 S. Kumar, V. Saini, I. K. Maurya, J. Sindhu, M. Kumari, R. Kataria and V. Kumar, Design, synthesis, DFT, docking studies and ADME prediction of some new coumarinyl linked pyrazolylthiazoles: Potential standalone or adjuvant antimicrobial agents, *PLoS One*, 2018, **13**(4), 0196016.

77 F. Pereira, K. Xiao, D. A. Latino, C. Wu, Q. Zhang and J. Aires-de-Sousa, Machine learning methods to predict density functional theory B3LYP energies of HOMO and LUMO orbitals, *J. Chem. Inf. Model.*, 2017, **57**(1), 11–21.

78 R. Vijayaraj, V. Subramanian and P. Chattaraj, Comparison of global reactivity descriptors calculated using various density functionals: a QSAR perspective, *J. Chem. Theory Comput.*, 2009, **5**(10), 2744–2753.

79 R. G. Parr and R. G. Pearson, Absolute hardness: companion parameter to absolute electronegativity, *J. Am. Chem. Soc.*, 1983, **105**(26), 7512–7516.

80 P. Geerlings, F. De Proft and W. Langenaeker, Conceptual density functional theory, *Chem. Rev.*, 2003, **103**(5), 1793–1874.

81 R. G. Parr, L. v. Szentpály and S. Liu, Electrophilicity Index, *J. Am. Chem. Soc.*, 1999, **121**(9), 1922–1924.

82 P. K. Chattaraj and S. Giri, Stability, Reactivity, and Aromaticity of Compounds of a Multivalent Superatom, *J. Phys. Chem. A*, 2007, **111**(43), 11116–11121.

83 R. Srivastava, Theoretical studies on the molecular properties, toxicity, and biological efficacy of 21 new chemical entities, *ACS Omega*, 2021, **6**(38), 24891–24901.

84 Z. He, J. Zhang, X. H. Shi, L. L. Hu, X. Kong, Y. D. Cai and K. C. Chou, Predicting drug-target interaction networks based on functional groups and biological features, *PLoS One*, 2010, **5**(3), e9603.

85 N. Flores-Holguín, J. Frau and D. Glossman-Mitnik, Computational prediction of bioactivity scores and chemical reactivity properties of the Parasin I therapeutic peptide of marine origin through the calculation of global and local conceptual DFT descriptors, *Theor. Chem. Acc.*, 2019, **138**, 1–9.

86 C. Cárdenas, N. Rabi, P. W. Ayers, C. Morell, P. Jaramillo and P. Fuentealba, Chemical reactivity descriptors for ambiphilic reagents: dual descriptor, local hypersoftness, and electrostatic potential, *J. Phys. Chem. A*, 2009, **113**(30), 8660–8667.

87 S. K. Saha, M. Murmu, N. C. Murmu and P. Banerjee, Evaluating electronic structure of quinazolinone and pyrimidinone molecules for its corrosion inhibition effectiveness on target specific mild steel in the acidic medium: a combined DFT and MD simulation study, *J. Mol. Liq.*, 2016, **224**, 629–638.

88 J. Hossen, M. A. Ali and S. Reza, Theoretical investigations on the antioxidant potential of a non-phenolic compound thymoquinone: a DFT approach, *J. Mol. Model.*, 2021, **27**(6), 173.

89 K. Kaavin, D. Naresh, M. R. Yogeshkumar, M. Krishna Prakash, S. Janarthanan, M. Murali Krishnan and M. Malathi, In-silico DFT studies and molecular docking evaluation of benzimidazo methoxy quinoline-2-one ligand and its Co, Ni, Cu and Zn complexes as potential inhibitors of Bcl-2, Caspase-3, EGFR, mTOR, and PI3K, cancer-causing proteins, *Chem. Phys. Impact.*, 2024, **8**, 100418.

90 T. Nishiyama, N. Hatae, T. Yoshimura, S. Takaki, T. Abe, M. Ishikura, S. Hibino and T. Choshi, Concise synthesis of carbazole-1,4-quinones and evaluation of their antiproliferative activity against HCT-116 and HL-60 cells, *Eur. J. Med. Chem.*, 2016, **121**, 561–577.

91 M. Tercel, H. H. Lee, S. Y. Mehta, J. J. Youte Tendoung, S. Y. Bai, H. S. Liyanage and F. B. Pruijn, Influence of a basic side chain on the properties of hypoxia-selective nitro analogues of the duocarmycins: Demonstration of substantial anticancer activity in combination with irradiation or chemotherapy, *J. Med. Chem.*, 2017, **60**(13), 5834–5856.

92 S. J. Choi, J. E. Lee, S. Y. Jeong, I. Im, S. D. Lee, E. J. Lee, S. K. Lee, S. M. Kwon, S. G. Ahn and J. H. Yoon, 5, 5′-substituted indirubin-3′-oxime derivatives as potent cyclin-dependent kinase inhibitors with anticancer activity, *J. Med. Chem.*, 2010, **53**(9), 3696–3706.

93 O. Noureddine, N. Issaoui and O. Al-Dossary, DFT and molecular docking study of chloroquine derivatives as antiviral to coronavirus COVID-19, *J. King Saud Univ. Sci.*, 2021, **33**(1), 101248.

94 A. Mubarik, S. Mahmood, N. Rasool, M. A. Hashmi, M. Ammar, S. Mutahir, K. G. Ali, M. Bilal, M. N. Akhtar and G. A. Ashraf, Computational Study of Benzothiazole Derivatives for Conformational, Thermodynamic and Spectroscopic Features and Their Potential to Act as Antibacterials, *Crystals*, 2022, **12**(7), 912.

95 S. Sakthivel, T. Alagesan, S. Muthu, C. S. Abraham and E. Geetha, Quantum mechanical, spectroscopic study (FT-IR and FT - Raman), NBO analysis, HOMO-LUMO, first order hyperpolarizability and docking studies of a non-

steroidal anti-inflammatory compound, *J. Mol. Struct.*, 2018, **1156**, 645–656.

96 M. Sankarganesh, J. D. Raja, N. Revathi, R. V. Solomon and R. S. Kumar, Gold (III) complex from pyrimidine and morpholine analogue Schiff base ligand: synthesis, characterization, DFT, TDDFT, catalytic, anticancer, molecular modeling with DNA and BSA and DNA binding studies, *J. Mol. Liq.*, 2019, **294**, 111655.

97 B. K. Paul and N. Guchhait, A spectral deciphering of the binding interaction of an intramolecular charge transfer fluorescence probe with a cationic protein: thermodynamic analysis of the binding phenomenon combined with blind docking study, *Photochem. Photobiol. Sci.*, 2011, **10**(6), 980–991.

98 V. T. Sabe, T. Ntombela, L. A. Jhamba, G. E. Maguire, T. Govender, T. Naicker and H. G. Kruger, Current trends in computer aided drug design and a highlight of drugs discovered via computational techniques: A review, *Eur. J. Med. Chem.*, 2021, **224**, 113705.

99 O. Trott and A. J. Olson, AutoDock Vina: improving the speed and accuracy of docking with a new scoring function, efficient optimization, and multithreading, *J. Comput. Chem.*, 2010, **31**(2), 455–461.

100 S. C. Palapetta, H. Gurusamy, S. Krishnan and S. Ponnusamy, Facile Multicomponent Synthesis, Computational, and Docking Studies of Spiroindoloquinazoline Compounds, *ACS Omega*, 2022, **7**(9), 7874–7884.

101 V. Asati, D. K. Mahapatra and S. K. Bharti, PI3K/Akt/mTOR and Ras/Raf/MEK/ERK signaling pathways inhibitors as anticancer agents: Structural and pharmacological perspectives, *Eur. J. Med. Chem.*, 2016, **109**, 314–341.

102 M. E. Salem, M. Samir, A. H. Elwahy, A. M. Farag, A. M. Selim, A. A. Alsaegh, M. Sharaky, N. Bagato and I. T. Radwan, Design, synthesis, docking study, cytotoxicity evaluation, and PI3K inhibitory activity of Novel di-thiazoles, and bis (di-thiazoles), *J. Mol. Struct.*, 2024, **1301**, 137379.

103 M. Yu, Q. Gu and J. Xu, Discovering new PI3Kα inhibitors with a strategy of combining ligand-based and structure-based virtual screening, *J. Comput.-Aided Mol. Des.*, 2018, **32**(2), 347–361.

104 P. Chen, Y. L. Deng, S. Bergqvist, M. D. Falk, W. Liu, S. Timofeevski and A. Brooun, Engineering of an isolated p110α subunit of PI3Kα permits crystallization and provides a platform for structure-based drug design, *Protein Sci.*, 2014, **23**(10), 1332–1340.

105 G. M. Sastry, M. Adzhigirey, T. Day and R. Annabhimoju, Ligand preparation: parameters, protocols, and influence on virtual screening enrichments, *J. Comput.-Aided Mol. Des.*, 2013, **27**, 221–234.

106 J. Wang, P. A. Kollman and I. D. Kuntz, Flexible ligand docking: a multistep strategy approach, *Proteins: Struct., Funct., Bioinf.*, 1999, **36**(1), 1–19.

107 Systèmes, D., *Biovia, Discovery Studio Modeling Environment*, Dassault Systèmes Biovia, San Diego, CA, USA, 2016.

108 Biovia, D. S., *Discovery Studio*, Dassault Systèmes BIOVIA, 2016.

109 A. Singh, K. Kaur, H. Kaur, P. Mohana, S. Arora, N. Bedi, R. Chadha and P. M. S. Bedi, Design, synthesis and biological evaluation of isatin-benzotriazole hybrids as new class of anti-Candida agents, *J. Mol. Struct.*, 2023, **1274**, 134456.

110 M. Caricato, M. J. Frisch, J. Hiscocks and M. J. Frisch, *Gaussian 09: IOps Reference*, Gaussian Wallingford, CT, USA, 2009.